2008

Friction stir spot welding of aluminum alloys

Wei Yuan

Department:

Recommended Citation

FRICTION STIR SPOT WELDING

OF ALUMINUM ALLOYS

by

WEI YUAN

A THESIS

Presented to the Faculty of the Graduate School of the

MISSOURI UNIVERSITY OF SCIENCE AND TECHNOLOGY

In Partial Fulfillment of the Requirements for the Degree

MASTER OF SCIENCE IN MATERIALS SCIENCE AND ENGINEERING

2008

Approved by

Rajiv S. Mishra, Advisor
F. Scott Miller
Lokesh R. Dharani

PUBLICATION THESIS OPTION

This thesis consists of the following two articles that have been prepared for submission for publications as follows:

Page 20-42 are intended for submission to the MATERIALS SCIENCE AND ENGINEERING A.

Page 43-62 are intended for submission to the SCIENCE AND TECHNOLOGY OF WELDING AND JOINING.

ABSTRACT

Efforts to reduce vehicle weight and improve safety performance have resulted in increased application of light-weight aluminum alloys and a recent focus on the weldability of these alloys. Friction stir spot welding (FSSW) is a solid state welding technique (derivative from friction stir welding (FSW), which was developed as a novel method for joining aluminum alloys). During FSSW, the frictional heat generated at the tool-workpiece interface softens the surrounding material, and the rotating and moving pin causes material flow. The forging pressure and mixing of the plasticized material result in the formation of a solid bond region.

The present work investigated the effect of tool designs and process parameters on microstructure and mechanical properties of friction stir spot welds. Different tool designs were compared and process parameters were optimized for specific aluminum alloy 6016 (AA6016) based on lap-shear test. Effect of paint-bake cycle on weld properties was also studied. Different failure modes for welds were proposed and discussed.

Material flow during FSSW using a step spiral pin was studied by decomposing the welding process and examining dissimilar alloys spot welds which allowed a visualization of material flow based on their differing etching characteristics. The formation and control of a skew "Y" shape oxide layer was investigated. The movement of upper and bottom sheet material, and their mixing during FSSW were observed.

ACKNOWLEDGMENTS

I would like to thank my advisor, Dr. Rajiv S. Mishra, for giving me a great opportunity to work in this innovative research area. I am grateful to him for giving me continuous support, guidance and encouragement in this endeavor. His knowledge and patience encouraged me through the journey of my research. I would also like to acknowledge NSF I/UCRC program for providing the funding.

I am grateful to my committee members, Dr. F. Scott Miller and Dr. Lokesh R. Dharani for their valuable suggestions and inputs for this work.

I would also like to take this opportunity to extend my sincere thanks to all my present and former colleagues. I am especially grateful to Manasij Yadava and Kamini Gupta for their valuable suggestions and assistance. I am also grateful to Dr. Wang, Dr. Dutta, Saumydeep Jana, Partha De, Jeff Rodelas, Gaurav Bhargava, Bharat Gattu, Arun Mohan, Nilesh Kumar, Jiye Wang, Gaurav Argade, Abhilash Raveendranathan, Tim Freeney, Neal Ross, Prabhanjana Kalya, Nagarajan Balasubramanian, Marco Garcia and Steve Webb.

This thesis is dedicated to my dearest parents, my sister and friends who stood by me, encouraged me to pursue my dreams and expected great things for me.

TABLE OF CONTENTS

SECTION

LIST OF ILLUSTRATIONS

PAPER II

LIST OF TABLES

1. INTRODUCTION

Weight reduction without affecting the safety performance is a great challenge in the automotive industry in order to improve fuel economy and reduce emissions. It has been reported that fuel consumption can be reduced by 5.5% for each 10% reduction in vehicle weight and a one-pound reduction in the weight of a car would reduce carbon dioxide emissions by 20 pounds over the life of the vehicle [1, 2]. An automobile consists of outer panels and a platform, which is typically made of steel and contains the drive system, engine system and exhaust system. The weight of the platform is around 70 % of the total weight of an automobile.

Steel has been applied widely in the automotive industry because of its wide range of desirable properties, ease of processing, availability, and recyclability. However, lightweight materials like aluminum have obvious advantages over steel with comparable properties but an almost three times lower density, a high corrosion resistance, and high degree of utilization reaching 85-95% [3]. Aluminum alloys are promising candidates for replacing equivalent steel assemblies and the use of them in the automotive industry is increasing recently.

For replacing steel with aluminum in the structure of automobiles, it is necessary to explore joining methods that can be used efficiently. Current panel welding techniques used to join steels include resistance spot welding (RSW) and self-piercing rivets (SPR). However, these welding techniques can not be applied easily to aluminum alloy, because of its physical properties, particularly surface oxide film. Friction stir spot welding (FSSW) is a derivative of friction stir welding, which was developed by TWI (Abington, United Kingdom) in 1991 as a solid-state method for aluminum alloy joining [4]. This

novel joining mechanism is advantageous for producing aluminum joints without contamination, blowholes, porosity and cracks.

1.1. ALUMINUM AND ITS 6XXX SERIES ALLOYS

Aluminum and its alloys have been used extensively in modern life, from soda cans, household cookers to automotive and aircraft structures. Low density, high strength, high ductility, excellent formability and high corrosion resistance in the ambient environment make them promising candidates for vehicles, particularly the closure panels such as hoods, decklids and lift-gates.

The weldability of aluminum alloys varies depending on the chemical composition of the alloy used. The 6XXX series aluminum alloys mainly used in this project, designating the Al-Mg-Si-(Cu) alloys, are most commonly used for extrusion purpose and are widely used as automobile body sheets. This 6XXX series alloys are heat-treatable and have the following qualities:

> ➢ Good corrosion resistance
> ➢ Perfect surface finish
> ➢ Good formability
> ➢ Medium strength
> ➢ Hemming behavior
> ➢ Easy recyclability

All these advantages make them suitable for structural applications. Magnesium and silicon are the main additions and combine to form the stoichiometric compound, Mg_2Si, which makes 6XXX series alloys heat treatable and capable of achieving medium strength after artificial ageing. An increase in the Mg_2Si content results in improved tensile properties.

1.2. CONVENTIONAL WELDING METHODS FOR ALUMIUM ALLOYS

A number of welding methods are available based on the variability associated with entities joined, corresponding joining mechanism and source of energy used. Conventional methods used for aluminum alloy welding in automotive industry are resistance spot welding (RSW) and self-piercing riveting (SPR).

1.2.1. Resistance Spot Welding

RSW is one of a group of resistance welding (RW) process, in which workpieces are welded due to a combination of pressure applied by electrodes and enormous amounts of heat, which is generated locally by a high electric current flowing through the contact area of the weld [5]. A schematic of resistance spot welding is shown in Fig. 1.1. Two electrodes are simultaneously used to clamp workpieces together and to pass current through them.
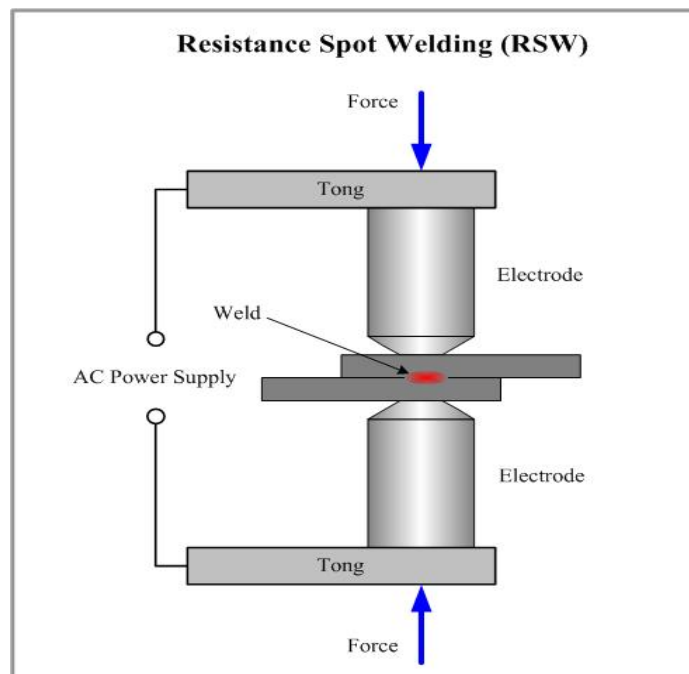
Fig. 1.1. A schematic of resistance spot welding [6].

The amount of heat delivered to the spot is determined by the resistance between the electrodes, the amplitude and duration of the current and the heat loss factor. The formula for heat generation during RSW is [5]:

$$H = I^2 RTK \tag{1.1}$$

where $I =$ Current flowing through the weld in amps

$R =$ Resistance in ohms from one electrode tip to the second tip

$T =$ Time of current flow in seconds

$K =$ Heat loss factor

The amount of energy needed to produce a sound weld varies with the change of sheet material properties, thickness, and type of electrodes. Either too little or too much heat will not give a good joint. Too little heat will result in lack of melting and make a poor weld. Too much heat will melt too much material and make a hole rather than a weld.

Currently, RSW is widely used in automotive industry for joining overlapping vehicle steel body parts of up to 3 mm thick with quality welds quickly and cheaply. It also shows some advantages, including limited workpiece deformation, high production rates and easy automation. However, RSW of aluminum alloy sheets has many disadvantages; high heat input, porosity, cracks [7, 8]. Also severe electrode tip wear problem has been encountered during RSW [9].

Because aluminum has better electrical and heat conductivity than steel [10], the basic consequence of modified Ohm's law (Equation 1.1) indicates that the heat needed to melt the aluminum has to be generated with higher amperage levels. It is reported that resistance spot welding machines with KVA (kilo Volt-Ampere) ratings much greater than 20 KVA are required to make sound welds on most aluminum materials [5]. Welding machines must provide high currents and exact pressures in order to melt the aluminum and produce a sound weld, however, these accelerate the tip wear of electrode.

RSW includes melting and solidification process, aluminum alloys should also be cleaned prior to RSW, with the goal of removing oxides and oils from the surface to be welded. This is especially important because aluminum welds are susceptible to porosity due to hydrogen and dross due to oxygen [11]. Aluminum alloys are also susceptible to hot cracking, though preheating reduces the temperature gradient across the weld zone and thus helps reduce hot cracking, but it can reduce the mechanical properties of the weld material.

1.2.2. Self-Piercing Riveting

SPR is a high-speed mechanical cold joining process used to join two or more overlapping sheets by pushing a rivet through the stack from one side without pre-drilling holes to the sheets. A large-deformation process is involved during piercing.

Fig. 1.2 shows a schematic of SPR process. The self-piercing rivet, under the press applied by the punch, pierces the upper sheet and flare into the bottom sheet under the influence of an upset die. A mechanical interlock was formed between the rivet and the transformed sheets. The rivet stays in a position with its upper surface at the same level as the surface of the upper sheet [12]. This joining process comprises many pairs of contacts between the punch, holder, rivet, upper sheet, bottom sheet, and die.
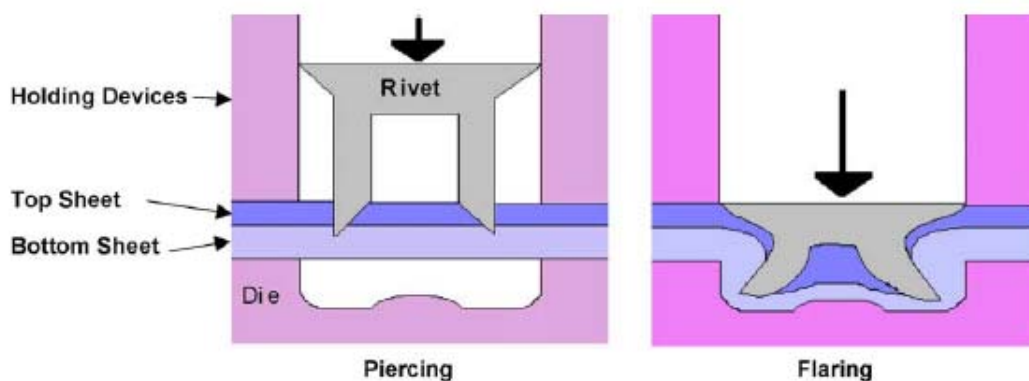
Fig. 1.2. An illustration of a self-piercing riveting process in cross section view [12].

Unlike RSW, no metallurgical process is involved in SPR joining, a wide range of materials can be joined, including combinations of similar or dissimilar materials, such as aluminum to aluminum, steel to steel and aluminum to steel. SPR shows better performance in joining aluminum alloys than RSW, it is environmentally friendly due to the low energy requirement, no fumes and low-noise emissions [13]. SPR of aluminum alloys also gives superior fatigue behavior than RSW of aluminum alloys [14].

The nature of this cold joining technique requires high forces be applied during the riveting process, which means machines must be built with the ability to handle massive loads. The ongoing piece cost of the rivets and the limited range of joint configurations are the main limitations [15]. The use of steel as reinforcement in aluminum body structure has raised corrosion concerns due to galvanic effects. Though this corrosion can be prevented by coating, the effect of cost on the quality and behavior of SPR joints can not be ignored [13].

1.3. FRICTION STIR SPOT WELDING

Recently, a new solid state welding technique, friction stir spot welding (FSSW) has been developed by Mazda Motor Corporation and Kawasaki Heavy Industry, as an extension of friction stir welding (FSW) for joining aluminum alloys [16, 17]. Mazda reported a great reduction in energy consumption and equipment investment compare to RSW for aluminum [18]. Since FSSW is a solid state welding process, no compressed air and coolant are need, and less electricity is required than RSW. Friction stir spot welds have higher strength, better fatigue life, lower distortion, less residual stress and better corrosion resistance.

Unlike FSW, there is no traverse movement after plunging a rotating non-consumable tool into the workpieces. Tools used for FSSW have two parts, a pin and a shoulder. The

pin is designed to disrupt the faying surface of the workpieces, shear and transport the material around it and produce deformational and frictional heat in the thick workpieces. The tool shoulder produces a majority of frictional heat to the surface and subsurface regions of the workpieces. Also the shoulder constrains the flow of plasticized material and produces the downward forging action [19].

1.3.1. Plunge Type FSSW

Plunge type FSSW is most commonly used in current industries. During plunge type FSSW, a rotation tool with a protruded pin is plunged into the workpieces from the top surface to a predetermined depth, and after a certain dwell time, it is retracted and a key hole is left. The frictional heat generated at the tool-workpiece interface softens the surrounding material, and the rotating and moving pin causes the material flow in both the circumferential and axial directions. The forging pressure applied by tool shoulder and mixing of the plasticized material result in the formation of a solid bond region. A schematic of plunge type FSSW method is indicated in Fig. 1.3.
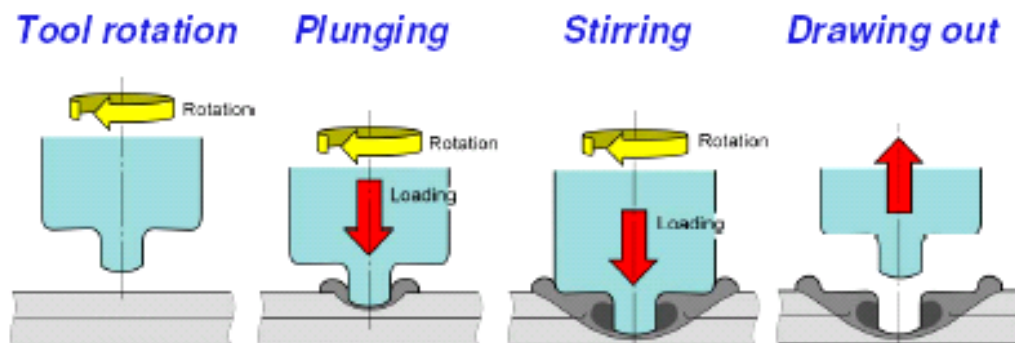
Fig. 1.3. A schematic of a plunge type FSSW [20].

1.3.2. Refill FSSW

Refill FSSW, which is a patented process of GKSS that joins two or more sheets of material together by utilizing delicate relative motions of the pin and the shoulder to fill

the pin hole [21, 22]. As indicated in Fig. 1.4, it consists of three stages: initiation, full plunge and full retract. In the initiation stage both the pin and shoulder are placed on the surface of upper sheet and rotate to generate sufficient frictional heat for plunging. The full plunge stage consists of plunging the shoulder into the sheet material and retracting the pin. In the full retract stage, the shoulder is retracted and pin is plunged to push the displaced material back into the void formed by the shoulder [23].
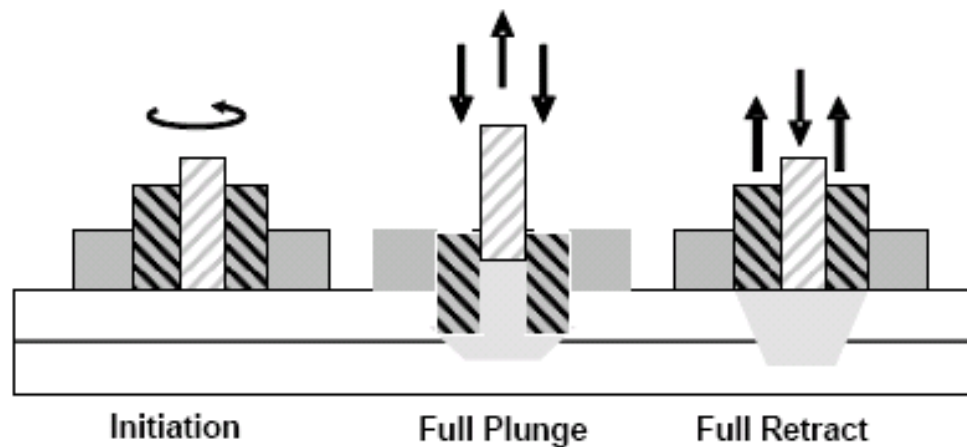
Fig. 1.4. Schematic of refill FSSW process [24].

A modified Refill FSSW process, called fixed-position refill FSSW, was developed in the Advanced Materials Processing and Joining Laboratory of South Dakota School of Mines [22]. Instead of plunging shoulder into the sheet material, a pin plunge into the sheets method was employed. As shown in Fig. 1.5, during Stage 1, the rotating pin and shoulder move towards the sheets. In the Stage 2, the pin plunges to the desired depth and the shoulder reservoir fills with the displaced material. Then the pin is retracted into the shoulder while the shoulder extrudes the displaced material back into the void left as the pin is retracted. At last stage, the shoulder and pin are retracted after some dwell time [24].
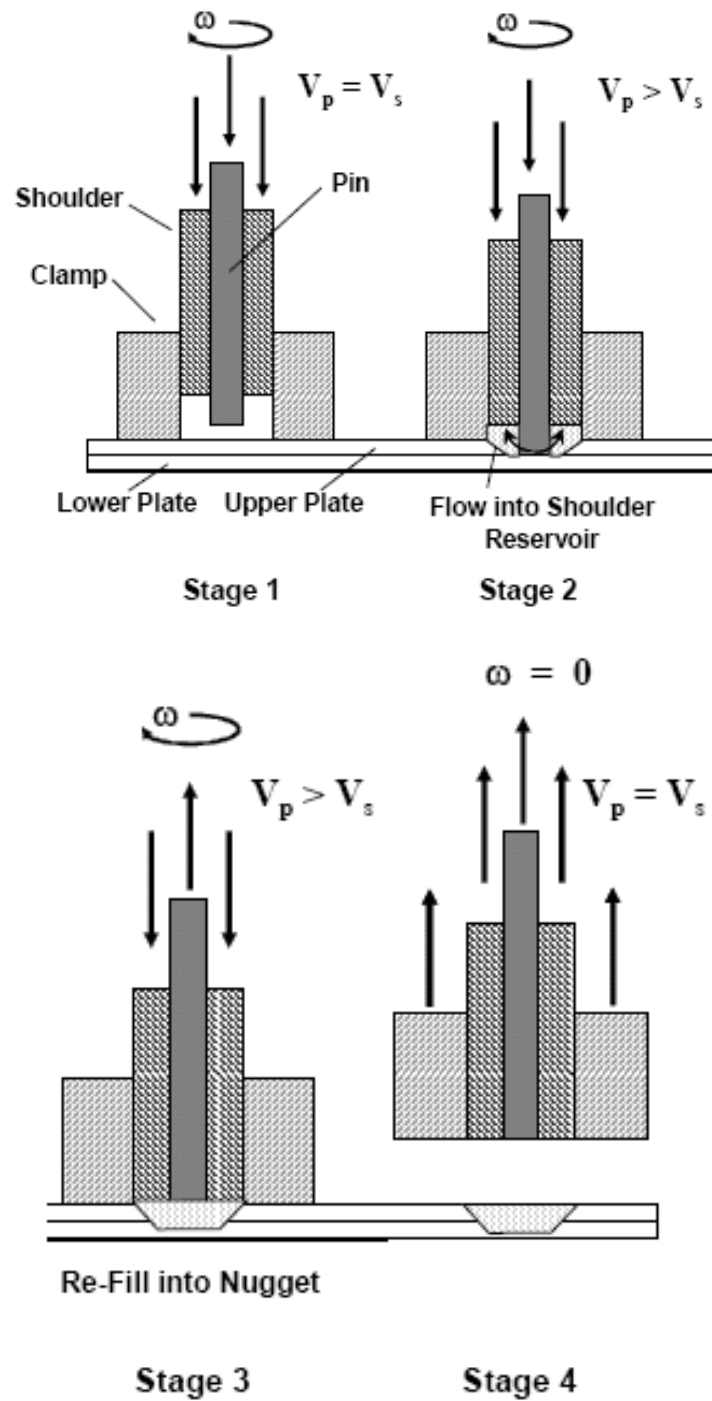
Fig. 1.5. Stages of the modified refill FSSW process [24].

1.3.3. Stitch FSSW

Another variation of the FSSW is "stitch FSSW" from GKSS [20], as illustrated in Figure 1.6. During stitch FSSW, the tool, after plunging, traverses a short linear distance before retracting. The purpose of this method is to produce joints with larger joining area for higher strength.
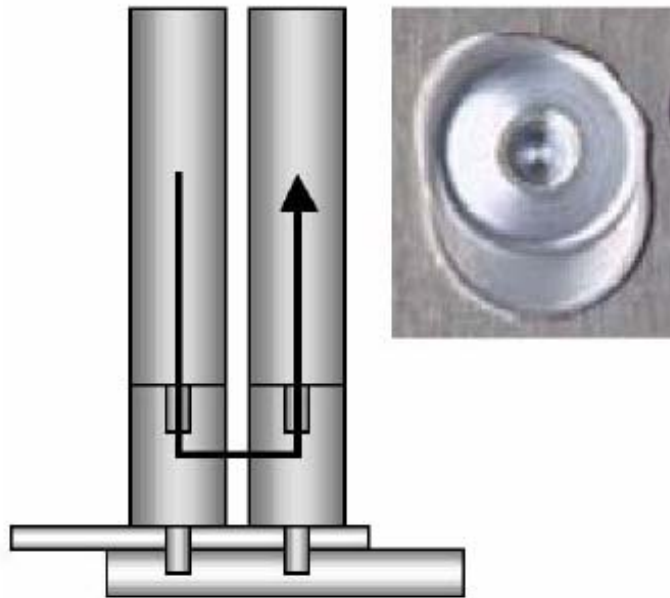
Fig. 1.6. Schematic of stitch FSSW [20].

1.3.4. Swing FSSW

Swing FSSW was developed out of stitch FSW by Hitachi [25] with the idea to give a large enough radius. As shown in Fig. 1.7, after plunging, the tool goes up a little but this is negligible since it moves in a swing-like motion with large radius and small angle [25]. This movement results in squeezed material located at the end of the welding.

The plunge type FSSW requires the simplest gun or assembly with spindle motor and tool plunge motor. An additional motor is needed to give a linear movement for stitch FSSW, which leads to complex and heavy C-frame gun design. A prototype C-frame

"swing stir" gun has been designed by Hitachi. As shown in Fig.1.8, it consists of three motors: the spindle motor for tool rotation, a tool plunge motor and a swing motor for the sliding cam used to swing the rotating tool in an arc giving a swing motion.
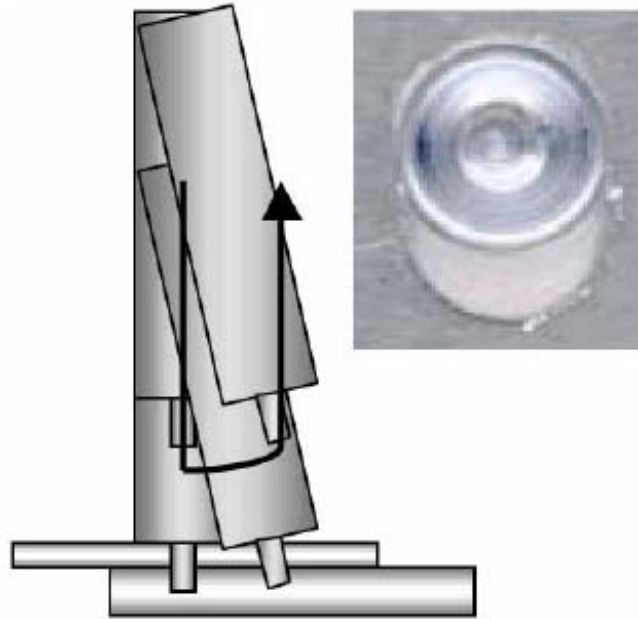
Fig. 1.7 Schematic of swing FSSW [25].
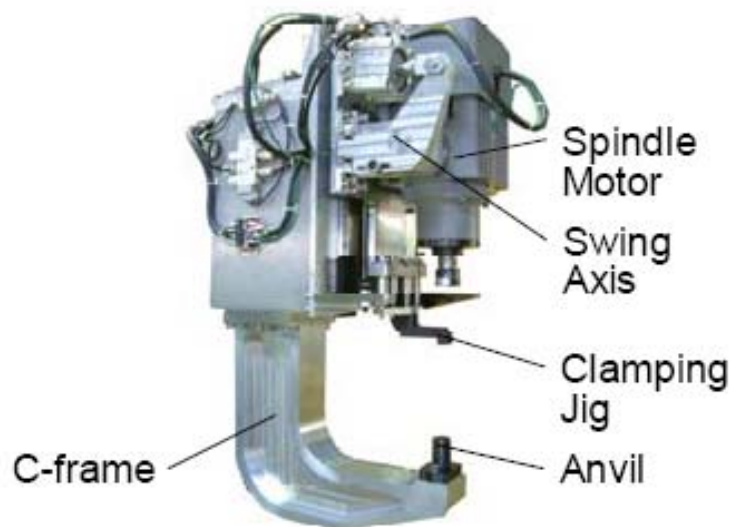
Fig. 1.8 Prototype swing FSSW gun "Swing-Stir" [25].

1. 4. FSSW VS. CONVENTIONAL WELDING

FSSW is a derivative of the FSW process. It has been used in the production of aluminum doors, engine hoods, and decklids in the automotive industry [20]. Mazda has claimed the benefits of using FSSW of aluminum for RX-8 production [26]. Compared to the conventional welding process, such as RSW and SPR, it has following benefits:

➢ High joint strength without porosity, cracks and contamination. There is no material melting during FSSW.

➢ Lower energy consumption. The only energy consumed in FSSW is the electricity needed to rotate and drive the tool. Compared to RSW, the energy consumption has reduced by 99% for FSSW of aluminum and 80% for steel [26].

➢ Lower equipment investment. About 40% reduction in equipment investment compared to RSW for aluminum is reported [18]. No large-scale electricity supply is required and tools for FSSW are no-consumable.

➢ No hazardous emissions and environment friendly. No weld spatter, noise and reduced vapor emissions during FSSW.

➢ Little welding deformation. FSSW is a solid state welding process without melting of materials, so distortions are smaller than for RSW and SPR.

➢ High repeatability and consistence due to its simple joining mechanism with few process parameters.

➢ Lower maintenance. Since equipment used is less than that used for RSW and SPR.

➢ No preparation and consumables are needed. Such as surface clean, drilling, and rivets or bolts.

1.5. TOOL DESIGN FOR FSSW

Friction stir spot welding tool consists of a tool shoulder and a pin. Shoulder produces a majority of the deformational and frictional heat to the surface and subsurface regions and applies a forging pressure to welds, while the pin produces a majority of the heat in the thick workpieces and transports the material around it. Different tool designs will modify their effects on weld properties.

Lin et al. [27, 28] compared effects of concave and flat shoulder on lap-shear strength and fatigue life of welds and indicated that welds made using concave shoulder had higher shear strength and fatigue life. Su et al. [29, 30] studied three different tool designs: a tool with threaded pin and shoulder, a tool with smooth pin and shoulder, and a tool with only smooth pin. They reported very small amount of the energy of FSSW was used to form the stir zone and thread on the pin had negligible influence on the energy generated during FSSW when compared to smooth pin. Tozaki et al. [31] used tools with three different pin lengths to study their effects on static strength. They reported tensile shear strength increased with increasing pin length when keeping the shoulder penetration depth same.

1.6. MECHANICAL PROPERTIES OF FRICTION STIR SPOT WELDS

The most commonly used testing methods to determine the properties of spot welds are lap-shear tension test, cross-tension test, fatigue test and microhardness. Lap-shear test is a fast, convenient and practical method for evaluating weld property. This test was used in almost all current literature when considering the mechanical properties.

Tozaki et al. [31] studied the effect of pin length on cross-tension strength of AA6016-4 spot weld and indicated that strength was not affected significantly by pin length. While cross-tension strength for dissimilar spot welds of AA2017-T6 to AA5052 decreased

with increasing tool rotation speed and tool holding time [32]. Lin et al. [27, 28] studied the fatigue properties of AA6111-T4 spot welds and indicated quite different failure modes for welds made using flat and concave tool shoulder.

1.7. MATERIAL FLOW AND SIMULATION

"Hooking" feature at the interface of the weld is shown in most of the current literature. The feature indicates material flow during FSSW and always affects the weld properties. Freeney et al. [33] studied the material flow of AA5052 spot welds and indicated that upward curve interface gave low lap-shear strength and relatively flat interface gave higher strength.

Su et al. [34] analyzed the material flow during spot welding of dissimilar AA5754/AA6111 and indicated a downward material flow close to the pin and an upward material flow further from the pin periphery. Tozaki [32] also provided a similar schematic illustration of this material flow during spot welding of dissimilar AA 2017-T6/AA5052. Muci-Kuchler et al. [35] analyzed the material flow during refill type FSSW and indicated the material located directly underneath the pin or in contact with the pin surface experienced a significant stirring motion. In addition, some computational methods including FEA have been also used to model the material flow [36-40].

1.8. FSSW OF MAGNESIUM ALLOYS AND ALUMINUM TO MAGNESIUM ALLOYS

FSW of several kinds of the automotive magnesium alloys and the dissimilar material joining of magnesium to aluminum alloys has been studied. Butt welded magnesium alloys of wrought and die-cast show advantages expected of the FSW process [41]. Gerlich et al. [42] studied the peak temperature during FSSW of AZ91 and indicated this peak temperature was 0.99 times of the melting temperature. Su et al. [43] investigated

spot welding of as-cast AZ91D and thixomolded AZ91 and reported the formation of local melted film during FSSW. The mechanical properties of dissimilar FSSW of AA5754 to AM60 were investigated by Su et al. [44] and results indicated fracture load increased when the projected bonded area immediately adjacent to the keyhole periphery and the energy input during welding increased.

1.9. JUSTIFICATION AND PROBLEM

The properties of friction stir spot welds vary greatly depending on tool design, welding process parameters, and material needs to be welded. These make it difficult to achieve optimized properties for a specific material. Tool design plays an important role in achieving high strength spot welds. A cylindrical or conical pin with or without threads are the most reported tool designs in current literatures. However, other pin designs are very limited and the comparison for tool designs is also limited. Lots of current literature has reported the analysis of process parameters on weld properties, but optimization for weld properties is seldom done.

Understanding how the material moves during different stages of FSSW is practically important and essential to achieve optimized welding parameters and obtain high efficiency welds. Material flow during FSSW has been reported in some literature. However, much more work is required to better understand the spot welding process.

1.10. RESEARCH OBJECTIVES AND METHODOLOGY

Based on these, my thesis consists of plunge type FSSW of aluminum alloys from two aspects. One aspect was to achieve optimized mechanical properties of spot welds and how the tool design, process parameters and paint-bake cycle (a kind of heat treatment at 170 °C for 20 minutes) affect these. The other aspect was to understand the material flow during FSSW.

In the first section, aluminum alloy 6016 (AA6016) was used and different tool designs were compared based on the size of bonded region, cross sectional welding features and lap-shear strengths. Process parameters were optimized based on the lap-shear failure load, the tool plunge force and spindle torque. Effect of paint-bake cycle on spot welds was investigated by using optimized process parameters. The failure mechanism of spot welds was also studied.

In the second section, material flow during FSSW when using a conventional step spiral pin tool was investigated by decomposing the welding process and examining dissimilar alloys spot welding (AA6016/AA5182) which allowed a visualization of material flow based on their differing etching.

1.11. BIBLIOGRAPHY

[1] I. J. Polmear, "Light alloys", Third edition, Edward Arnold (1995).

[2] I. Png, "Managerial economics", Blackwell Publishing, 3rd edition (2002).

[3] I. N. Fridlyander, V. G. Sister, O. E. Grushko, V. V. Berstenev, L. M. Sheveleva, L. A. Ivanova, Metal Science and Heat Treatment 44 (2002) 365-370.

[4] W. M. Thomas, E. D. Nicholas, J. C. Needham, M. G. Murch, P. Templesmith, C. J. Dawes, G. B. Patent 9125978.8 (1991).

[5] Handbook for resistance spot welding, http://www.millerwelds.com/pdf/Resistance.pdf.

[6] http://www.substech.com/dokuwiki/doku.php?id=resistance_welding_rw&Doku Wiki=d8f6c29962e5ece4564bc65ad4065b8a.

[7] A. Gean, S. A. Westgate, J. C. Kucza, J. C. Ehrstrom, Welding Journal 78 (1999) 80s-86s.

[8] P. H. Thornton, A. R. Krause, R. G. Davies, Welding Journal 75 (1996) S101-S108.

[9] M. I. Khan, M. L. Kuntz, P. Su, A. Gerlich, T. North, Y. Zhou, Science and Technology of Welding and Joining 12 (2007) 175-182.

[10] M. Yamamoto, A. Gerlich, T. H. North, K. Shinozaki, Journal of Materials Science 42 (2007) 7657-7666.

[11] http://en.wikipedia.org/wiki/Spot_welding.

[12] W. Cai, P. C. Wang, W. Yang, International Journal of Machine Tools & Manufacture 45 (2005) 695-704.

[13] L. Han, A. Chrysanthou, Materials & Design 29 (2008) 458-468.

[14] G. S. Booth, C. A. Olivier, S. A. Westgate, F. Liebrecht, S. Braunling, SAE Technical papers: 2000-01-2681.

[15] Paul Briskham, Nicholas Blundell, Li Han, R. Hewitt, K. Young, D. Boomer, SAE Technical papers: 2006-01-0774.

[16] R. Sakano, K. Murakami, K.Yamashita, T. Hyoe, M. Fujimoto, M. Inuzuka, U. Nagao, H. Kashiki, Proceedings of the Third International Symposium of Friction Stir Welding, Kobe, Japan (2001).

[17] T. Iwashita, Method and apparatus for joining, US Patent Issued on August 5 (2003)

[18] R. Hancock, WELDING JOURNAL (2004) 40-43

[19] C. B. Fuller, in: R.S. Mishra, M.W. Mahoney (Eds.), Friction Stir Welding and Processing, ASM International, Ohio, 2007, pp. 7-35.

[20] T.-Y. Pan, SAE Technical papers, 2007-01-1702.

[21] H. Badarinarayan, F. Hunt, K. Okamoto, in: R.S. Mishra, M.W. Mahoney (Eds.), Friction Stir Welding and Processing, ASM International, Ohio, 2007, pp. 235-272.

[22] S. Kalagara, K. H. Muci-Küchler, W. J. Arbegast, Friction Stir Welding and Processing IV, TMS, 2007.

[23] K. H. Muci-Küchler, S. S. T. Kakarla, W. J. Arbegast, C. D. Allen, SAE Technical papers, 2005-01-1260.

[24] C. D. Allen, W. J. Arbegast, SAE Technical papers, 2005-01-1252.

[25] K. Okamoto, F. Hunt, S. Hirano, SAE Technical papers, 2005-01-1254.

[26] "Mazda Develops World's First Aluminum Joining Technology Using Friction Heat", Mazda media release, February 27, 2003.

[27] P. C. Lin, J. Pan, T. Pan, International Journal of Fatigue 30 (2008) 74-89.

[28] P. C. Lin, J. Pan, T. Pan, International Journal of Fatigue 30 (2008) 90-105.

[29] P. Su, A. Gerlich, T. H. North, G. J. Bendzsak, Science and Technology of Welding and Joining 11 (2006) 163-169.

[30] P. Su, A. Gerlich, T. H. North, G. J. Bendzsak, SAE Technical paper, 2006-01-0917.

[31] Y. Tozaki, Y. Uematsu, K. Tokaji, International Journal of Machine Tools and Manufacture 47 (2007) 2230-2236.

[32] Y. Tozaki, Y. Uematsu, K. Tokaji, Fatigue & Fracture of Engineering Materials & Structures 30 (2007) 143-148.

[33] T. Freeney, S. R. Sharma, R. S. Mishra, SAE Technical paper (2006) 2006-01-0969.

[34] P. Su, A. Gerlich, T. H. North, G. J. Bendzsak, Science and Technology of Welding and Joining 11 (2006) 61-71.

[35] K. H. Muci-Kuchler, S. K. Itapu, W. J. Arbegast, K. J. Koch, SAE Technical paper (2005) 2005-01-3323.

[36] K. H. Muci-Küchler, S. S. T. Kakarla, W. J. Arbegast, C. D. Allen, SAE Technical paper (2005) 2005-2001-1260.

[37] M. Awang, V. H. Mucino, Z. Feng, S. A. David, SAE Technical paper (2005) 2005-2001-1251.

[38] Sri S. T. Kakarla, K. H. Muci-kuchler, W. J. Arbegast, C. D. Allen, TMS (2005) 213-220.

[39] S. Mandal, J. Rice, A. Elmustafa, Friction Stir Welding and Processing IV, TMS, 2007.

[40] H. Badarinarayan, F. Hunt, K. Okamoto, S. Hirasawa, Friction Stir Welding and Processing IV, TMS, 2007.

[41] K. Okamoto, F. Hunt, SAE Technical paper, 2005-01-0730.

[42] A. Gerlich, P. Su, T.H. North, G. J. Bendzsak, Materials Forum Vol 29 (2005).

[43] P. Su, A. Gerlich, M. Yamamoto, T. H. North, Journal of Materials Science 42 (2007) 9954-9965.

[44] P. Su, A. Gerlich, T. H. North, SAE Technical paper (2005) 2005-2001-1255.

I. EFFECT OF TOOL DESIGN AND PROCESS PARAMETERS ON PROPERTIES OF FRICTION STIR SPOT WELDS

W. Yuan and R.S. Mishra[*]

Center for Friction Stir Processing, Department of Materials Science and Engineering

Missouri University of Science and Technology, Rolla, MO 65409, USA

(Prepared for publishing in Materials Science and Engineering A Journal)

ABSTRACT

Friction stir spot welding (FSSW) of 6016-T4 aluminum alloy sheet was evaluated with conventional pin (CP) tool and off-center feature (OC) tool. Tool rotation speed, plunge depth, plunge speed and dwell time were varied to determine the effect of individual process parameter on lap-shear failure load. Maximum failure load of about 3.3 kN was obtained by using 0.5 mm/s plunge speed, 0.2 mm shoulder penetration depth and 490 ms dwell time, 1500 rpm tool rotation speed for CP tool and 2500 rpm for OC tool. After paint-bake cycle, weld strength increased by 20.8% and 15.4%, respectively, for CP tool and OC tool. The OC tool exhibited much lower plunge force and torque. Three different failure modes of welds under lap-shear loading were observed: interfacial failure, nugget fracture failure and upper sheet fracture failure. Microhardness profile for weld cross section indicated no direct relationship between microhardness distribution and failure locations.

* Corresponding author. Tel: +01 573 341 6361 fax: +01 573 341 6934 E-mail: rsmishra@mst.edu (R.S. Mishra)

1.1. INTRODUCTION

Weight saving in the automotive industry is becoming increasingly important and can be enhanced by using light-weight aluminum alloy for vehicles; particularly closure panels such as hoods, decklids and lift-gates. Resistance spot welding (RSW), currently the most commonly used joining technique in the vehicle industry, has applications for low-carbon, high-strength and coated steels. However, RSW of aluminum alloy sheets is fraught with many disadvantages, which include porosity and cracks, as reported by Gean et al. [1] and Thornton et al. [2]. A severe electrode tip wear problem has also been encountered during RSW [3]. Recently, friction stir spot welding for joining aluminum alloy sheet has been developed by Mazda Motor Corporation and Kawasaki Heavy Industry [4, 5].

Similar to friction stir welding (FSW), which was developed by TWI, UK in 1991 [6], FSSW is a solid-state welding technique. During plunge type FSSW, a rotating tool with a protruding pin is inserted into the overlapping sheets with a specific plunge speed, to a predetermined depth. After a certain dwell time, it is retracted and a keyhole is left. The frictional heat generated at the tool-workpiece interface softens the surrounding material, and the rotating and moving pin causes the material flow in both the circumferential and axial directions. The inter-mixing of the plasticized material and forging pressure applied by the tool shoulder result in the formation of a solid bond region [7, 8].

The strength of welds is critical when applying FSSW to load-bearing components. This strength is affected mainly by tool geometry and process parameters. Tool geometry, such as shoulder diameter and shape, pin shape, length, diameter and feature is a key parameter to affect heat generation and material flow [9]. Currently, a concave tool shoulder is the most common shoulder design in FSSW, though some flat tool shoulder also has been used [10-12]. The tool pin is designed to disrupt the faying surface,

transport and shear adjacent material and generate frictional heat in the thick sheet. The most current pin design in open literature is conventional cylindrical and conical pin with or without thread [7, 8, 13-16]. Valant et al. [17] and Y. Hovanski et al. [18] have reported a three-pin feature design and a tapered three-flat pin design. Recently, Mishra et al. [19] have reported the concept of OC tool to have better control over the material sweep during FSSW. Process parameters are also key factors that affect the strength of the weld joints. The literature on how these process parameters affect weld strength is limited [7, 8, 17, 20-22], and only a general comparison can be achieved because of different alloy use, varied alloy thickness and tool design.

In this paper, two different tools with the same shoulder diameter and concave shape but different pin features were compared. One was a conventional tool with a center conical threaded pin, and the other was a tool with three off-center hemispherical pin features. Lap-shear tests were used to investigate systematically the effect of individual process parameter on weld strength by varying tool rotation speed, plunge depth, plunge speed and dwell time. The effect of paint-bake cycle on weld strength was also evaluated. Cross section and microstructure of the welded and failed specimens were analyzed to outline the different failure modes under lap-shear tests.

1.2. EXPERIMENTAL PROCEDURES

AA6016-T4 sheet with 1 mm thickness was used in this study. AA 6016 is a low Cu, Mg-Si alloy that gained popularity as skin material for car body panels due to its desirable dent resistance and relatively high formability [23]. Aluminum sheets were sheared to a dimension of 127 mm long and 38.1 mm wide. Fig. 1.1 shows a lap-shear specimen used to investigate the strength of the welds. The specimen had a 38.1mm square overlap area.

A plunge type FSSW machine with axial load capacity of 22.2 kN and spindle rotation speeds up to 3000 rpm was used. The FSSW machine also had the capability to vary plunge speeds up to 25mm/s and dwell time to a maximum of 1470 milliseconds (ms). During the weld, axial force, torque and time were data logged.

One of the most important processing variables is tool geometry. For the welding process, tool features have significant influence on frictional heat, material flow, plunge force and spindle torque. Two different tools are shown in Fig. 1.2. CP tool, which is a conventional tool with a center pin, has a concave shoulder with 10 mm diameter, and a 1.51 mm long conical thread pin with root diameter of 4.5 mm and tip diameter of 3 mm. OC tool is the off-center feature tool with the same concave shoulder shape and diameter, and three off-center 0.8 mm long hemispherical pin features. Both tools were machined from Densimet tungsten alloy.

The spot welding machine was operated under position control mode. For OC tool, a stop-then-retraction mode was used. Welded specimens were made at various parameter combinations. Tool rotation speed, plunge speed and dwell time were varied, and included 1000, 1500, 2000 and 2500 rpm, 0.3, 0.5, 0.7, 1.0 and 2.5 mm/s and 245, 490 and 735 ms. A combination of 1500 rpm rotation speed, 0.5 mm/s plunge speed and 490 ms dwell time was employed to set the welding program for each tool. The plunge depth was determined by increasing depth until the shoulder touched the top sheet completely. After setting the program, a gradually increase in plunge depth was made to achieve any target depth.

An MTS testing machine was used to evaluate three lap-shear specimens for each welding condition, and a standard deviation of maximum failure loads was employed. The paint-bake cycle corresponded to holding at 170°C for 20 minutes and tested under

lap-shear loading condition. Two doublers were used to induce a pure shear to the interfacial plane, and specimens were pulled at a rate of 0.02 mm/s. In addition to mechanical testing, two welds in each condition were cross-sectioned and mounted for metallographic studies and microhardness tests. Samples were prepared and etched using a 5% HF reagent to determine weld morphology.

Microhardness tests were performed on cross sections of welds made by both tools. Vickers microhardness measurements were taken at 0.5 mm below the upper sheet surface with 1.0 mm interval using a diamond indenter with a 0.5 kgf load and 10 s dwell time. The samples were kept in a freezer between FSSW runs and microhardness tests.

1.3. RESULTS AND DISCUSSION

1.3.1. Macrostructure

Cross sections of welds show typical bonded regions of welds (Fig. 1.3). Figs. 1.3 (a) and (b) show the cross sections of welds made at 1500 rpm and 2500 rpm using CP tool with 0.5 mm/s plunge speed, 490 ms dwell time and the same target plunge depth. A larger bonded region was indicated at low rpm, with a relatively flat hooking defect. At higher rpm, the hooking defect tended to curve upwards on the outer edge of the nugget region, which in turn decreased the bonded region. Figs. 1.3 (c) and (d) are cross-sections of welds made at 1500 rpm and 2500 rpm using OC tool with 0.5 mm/s plunge speed, 490 ms dwell time and the same target plunge depth. Unlike the results for CP tool, the size of the bonded region increased for OC tool from 1500 rpm to 2500 rpm, during which higher frictional heat was generated. On the other hand, the upward hooking defect is not pronounced; the small volume of pin features and shallow tool plunge depth should be the reason.

It is worth mentioning that, displacement control mode and same target plunge depth were used, more actual penetration depths were achieved at higher rotation speeds. For higher rotation speed welding, higher temperature results in lower strength of aluminum alloy. Valant et al. [17] reported similar observation and indicated that position of the Z-axis servomotor, axial load on the Z-axis spindle and finite stiffness of the machine determined the actual tool penetration depth. Though a stop-then-retraction mode was used for the OC tool, the motor inertia and softer material around the pins were pulled out with a rotating tool, which left a hole in the weld center. Void shape in welds was also reported by Valant et al. [17].

1.3.2. Lap-shear Test

For the first set of runs, tool rotation speed was varied from 1000 rpm to 2500 rpm; while plunge depth, plunge speed and dwell time were kept constant. Fig. 1.4 shows the effect of rotation speed on lap-shear failure load. For CP tool, lap-shear failure load first increased then decreased as the rotation speed increased, with a peak load of 2.61 kN at 1500 rpm. However, for OC tool, the lap-shear failure load increased as the tool rotation speed increased, with maximum value of 2.97 kN at 2500 rpm. The variation in lap-shear failure load with tool rotation speed is related to the frictional heat and material flow change. Su et al. [24] have shown a positive correlation between the bonded area and lap-shear strength. Higher tool rotation speed is believed to generate more friction heat, which is beneficial for larger bonded region formation. The strength of the welds also depends on the extent and quality of the bonded region, the thickness of the top sheet at the outer circumference of the shoulder indentation, and hooking defect. The climbing hooking defect decreased the bonded region for CP tool at higher tool rotation speed. However, larger bonded region, sufficient top sheet thickness and relatively flat hooking defect made the welds stronger at higher tool rotation speed for OC tool. As expected, plunge force and spindle torque decreased as the tool rotation speed increased for both

tools, which is related to higher thermal input. OC tool showed lower spindle torque and plunge force than those for CP tool.

For the second set of runs, the plunge depth (pin penetration depth) was varied by increasing the depth by 1 mm increments. Considering the finite stiffness of the machine, actual plunge depth was measured by weld cross section. The tool rotation speed was 1500 rpm for CP tool and 2500 rpm for OC tool, while tool rotation speed and dwell time were kept constant and the same for both tools. Fig. 1.5 shows how plunge depth affects the failure load. Different plunge depth was adopted for two tools. High plunge depth has been reported to generate high weld strength [8, 10]. Current results indicated the same trend of failure load with plunge depth for welds made using both tools; first an increase, and then a decrease. A peak value of 3.31kN was observed for welds made using CP tool with a plunge depth of 1.72mm, corresponding to a 0.21mm shoulder penetration. For OC tool, a plunge depth of 1.03 mm, corresponding to 0.23 mm shoulder penetration, gave the highest failure load of 3.25 kN. Continually increasing the plunge depth decreased the lap-shear failure load of welds made using both tools because the top sheet under the outer circumference of the tool shoulder became the weakest load-bearing cross section.

No special spindle torque change was observed for CP tool as the plunge depth increased. However, for OC tool, the spindle torque increased when the plunge depth increased. Increase in plunge force was observed for both tools since the tool shoulder penetrated deeper. OC tool showed a much lower spindle torque and plunge force than CP tool.

For the third set of runs, the plunge speed of the tool was varied from 0.3 mm/s to 2.5 mm/s for CP tool and from 0.3 mm/s to 1 mm/s for OC tool; while the tool rotation speed, plunge depth and dwell time were kept constant for each tool. The results of the lap-shear

test are shown in Fig. 1.6. Both tools produced highest strength welds using 0.5 mm/s plunge speed. Higher plunge speed welding has been reported widely [8, 15-17] to result in a productivity advantage. However, current research reports a sacrifice of weld strength from higher plunge speed. At the same time, higher plunge force and torque were observed at higher plunge speed welding.

For the fourth set of runs, the dwell time was varied from 245 ms to 735 ms, while the tool rotation speed, plunge depth and plunge speed were kept constant as 1500 rpm, 1.72 mm and 0.5 mm/s for CP tool; and 2500 rpm, 1.03 mm and 0.5 mm/s for OC tool. Fig. 1.7 shows the effect of dwell time on lap-shear failure load. The variation of failure load was small and a relatively higher failure load was achieved at 490 ms dwell time. Even longer dwell time was not tried, because of weld zone pullout, which created a keyhole in the welds made using OC tool, and bottom sheet deformation and bending up for CP tool. Not much variation in torque and plunge force was observed during this dwell period.

The effect of paint-bake cycle on lap-shear failure load is shown in Fig. 1.8. The process parameters used were 1500 rpm, 1.72 mm, 0.5 mm/s and 490 ms for CP tool; and 2500 rpm, 1.03 mm, 0.5 mm/s and 490 ms for OC tool. A 20.8% and 15.4% increase of lap-shear failure load was achieved for CP tool and OC tool with maximum value of 4.0 kN and 3.7 kN, respectively.

1.3.3. Failure Modes of Welds under Lap-shear Loading Condition

The strength of welds depends not only on the size of the bonded region, but also on hooking defect and thickness of the top sheet at the outer circumference of the shoulder indentation. The weakest point, of course, is the location for failure. The failure mode of specimen changes when welding process parameters vary. Mitlin et al. [12] have indicated that tool pin penetration depth had a strong effect on the failure mode of welds.

Su et al. [24] have shown energy input during FSSW influenced the fracture mode during mechanical testing.

In this study, three different failure modes under lap-shear tests were observed. A schematic plot of failure modes for welds is shown in Fig. 1.9. For each failure mode, initial crack started from the faying surface depicted as point "O". Mode IF, interfacial failure, crack propagated along the hooking defect to point A, then along the circumference to A'. In this case, crack propagated parallel to the upper sheet surface and welds failed limited plasticity at the weld nugget and the failure load was low. Mode NF, nugget fracture failure, crack propagated following hooking defect into the stir zone and then propagated to point B; after that came to point B' along inner circumference or to B1, B2 then to C' along outer circumference. Mode USF, upper sheet fracture failure; in this case, much more frictional heat input generated a large bonded region and hooking defect merged into the nugget completely. When the crack reached the stir zone, it followed the boundary of thermomechanically affected zone (TMAZ) and nugget to the thinnest part of top sheet, where fracture happened at point C then propagated to point C' along the outer circumference of the shoulder indentation. In this case, welds displayed certain plasticity on deformation and failed with a higher failure load. Failure route of mode USF is shown in Fig. 1.10 with welds cross section indicated at different lap-shear testing extension. Broken samples after lap-shear test are shown in Fig. 1.11 and Fig. 1.12.

The maximum failure load was achieved under mode USF failure condition for welds made using both tools; failure mode did not change as tool penetration depth continued to increase. However, the maximum failure load decreased greatly, potentially because the thin upper sheet under the shoulder indentation became weakest and dominated the final failure. The relation between failure load and extension of welds made using CP tool and failed at different failure modes is shown in Fig. 1.13. The results indicated three failure

mode regions and two mode transition regions. As the failure mode shifted from IF to USF, the failure loads and extensions were at least doubled. As was mentioned above, the failure load increased after the paint-bake cycle; however, no obvious variation of extension was seen. This may result from material property improvement after the paint-bake cycle.

1.3.4. Microhardness Test

The tensile properties of the weld are dependent only on the strength distribution of weld when it is free of defects. To understand the relationship between strength distribution and failure locations, microhardness profiles for weld cross sections were achieved at three different shoulder penetration depths which corresponded to three failure modes. Microhardness test was performed 0.5 mm below the upper sheet surface. The results in Fig. 1.14 show a typical heat-affected zone (HAZ) which undergoes thermal cycles with lowest microhardness. The HAZ moved away from the weld center resulting from higher thermal input as the shoulder penetration depth increased. No direct relationship between microhardness and failure locations was observed, since the microhardness increased when close to the weld center and there was not much variation in microhardness in nuggets as penetration depth increased; however, the failure location shifted away from the weld center with increase of penetration depth.

1.4. CONCLUSIONS

AA 6016 sheets were friction stir spot welded by using CP tool and OC tool. Results indicated that tool rotation speed and plunge depth profoundly influenced lap-shear failure load of welds, while plunge speed and dwell time had little effect. Both tools exhibited maximum weld failure load: About 3.3 kN at 0.5 mm/s plunge speed, 0.2 mm shoulder penetration depth and 490 ms dwell time; different tool rotation speeds, 1500 rpm for CP tool and 2500 rpm for OC tool. After the paint-bake cycles, weld strength

increased by 20.8% and 15.4%, respectively, for CP tool and OC tool. The OC tool displayed much lower plunge force and torque. Three different failure modes were observed for welds made using both two tools, interfacial failure, nugget fracture failure and upper sheet fracture failure. Microhardness test indicated no direct relationship between microhardness and failure modes, and HAZ was the softest region.

1.5. ACKNOWLEDGMENTS

1.6. REFERENCES

[1]   A. Gean, S.A. Westgate, J.C. Kucza, J.C. Ehrstrom, Welding Journal 78 (1999) 80s-86s.

[2]   P.H. Thornton, A.R. Krause, R.G. Davies, Welding Journal 75 (1996) S101-S108.

[3]   M.I. Khan, M.L. Kuntz, P. Su, A. Gerlich, T. North, Y. Zhou, Science and Technology of Welding and Joining 12 (2007) 175-182.

[4]   R. Sakano, K. Murakami, K. Yamashita, T. Hyoe, M. Fujimoto, M. Inuzuka, U. Nagao, H. Kashiki, Proceedings of the Third International Symposium of Friction Stir Welding, Kobe, Japan (2001).

[5]   T. Iwashita, Method and apparatus for joining, US Patent Issued on August 5 (2003).

[6]   W.M. Thomas, E.D. Nicholas, J.C. Needham, M.G. Murch, P. Templesmith, C.J. Dawes, G.B. Patent 9125978.8 (1991).

[7]   T. Freeney, S.R. Sharma, R.S. Mishra, SAE International, 2006-01-0969 (2006).

[8]   S. Lathabai, M.J. Painter, G.M.D. Cantin, V.K. Tyagi, Scripta Materialia 55 (2006) 899-902.

[9] R.S. Mishra, Z.Y. Ma, Materials Science and Engineering: R: Reports 50 (2005) 1-78.

[10] S.G. Arul, T.-Y. Pan, P.-C. Lin, J. Pan, Z. Feng, M.L. Santella, SAE International, 2005-01-1256 (2005).

[11] P.C. Lin, J. Pan, T. Pan, International Journal of Fatigue 30 (2008) 90-105.

[12] D. Mitlin, V. Radmilovic, T. Pan, J. Chen, Z. Feng, M.L. Santella, Materials Science and Engineering a-Structural Materials Properties Microstructure and Processing 441 (2006) 79-96.

[13] Y. Tozaki, Y. Uematsu, K. Tokaji, International Journal of Machine Tools and Manufacture 47 (2007) 2230-2236.

[14] D.A. Wang, S.C. Lee, Journal of Materials Processing Technology 186 (2007) 291-297.

[15] P. Su, A. Gerlich, T.H. North, G.J. Bendzsak, Science and Technology of Welding and Joining 11 (2006) 61-71.

[16] A. Gerlich, P. Su, T.H. North, Journal of Materials Science 40 (2005) 6473-6481.

[17] M. Valant, E. Yarrapareddy, R. Kovacevic, International Trends in Welding Research Conference, May 16-20 (2005).

[18] Y. Hovanski, M.L. Santella, G.J. Grant, Scripta Materialia 57 (2007) 873-876.

[19] R.S. Mishra, T.A. Freeney, S. Webb, Y.L. Chen, D.R. Herling, G.J. Grant, Friction Stir Welding and Processing IV, TMS (2007).

[20] Y. Tozaki, Y. Uematsu, K. Tokaji, Fatigue & Fracture of Engineering Materials & Structures 30 (2007) 143-148.

[21] H. Badarinarayan, F. Hunt, K. Okamoto, in: R.S. Mishra, M.W. Mahoney (Eds.), Friction Stir Welding and Processing, ASM International, Ohio, 2007, pp. 235-272.

[22] L. Fratini, A. Barcellona, G. Buffa, D. Palmeri, Proceedings of the Institution of Mechanical Engineers Part B-Journal of Engineering Manufacture 221 (2007) 1111-1118.

[23] S.M. Hirth, G.J. Marshall, S.A. Court, D.J. Lloyd, Materials Science and Engineering A 319-321 (2001) 452-456.

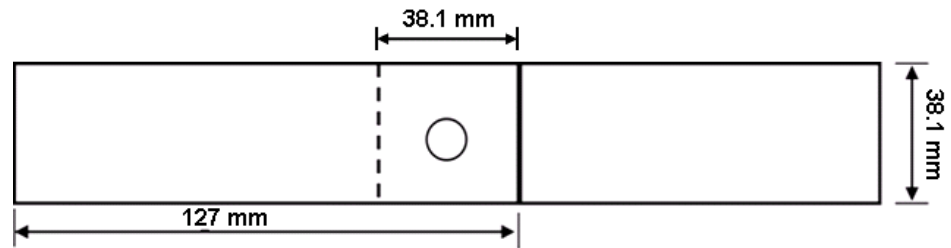[24] P. Su, A. Gerlich, T.H. North, SAE International, 2005-01-1255 (2005).

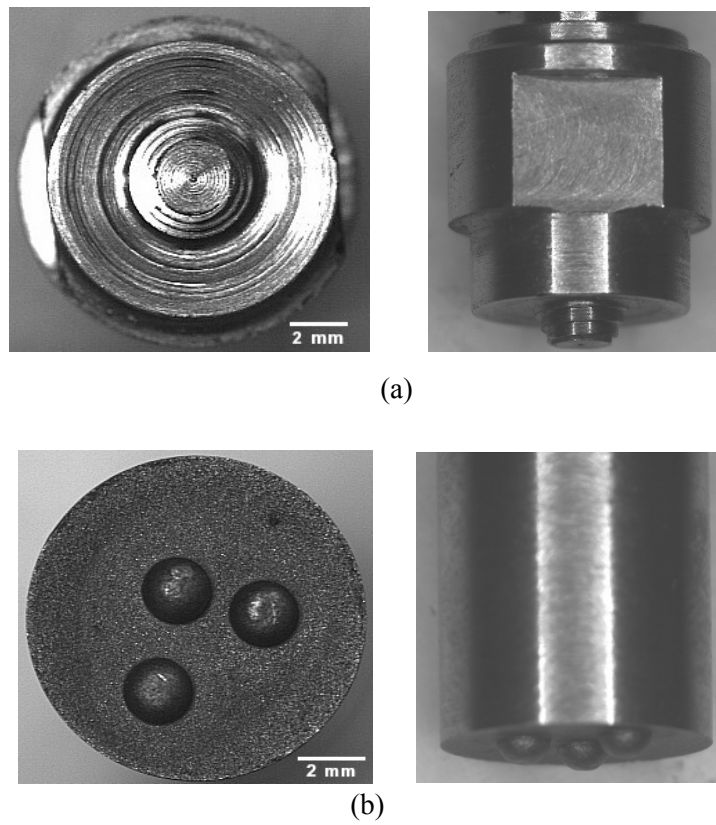Fig. 1.1. Schematic illustration of lap-shear specimen.

(a)

(b)

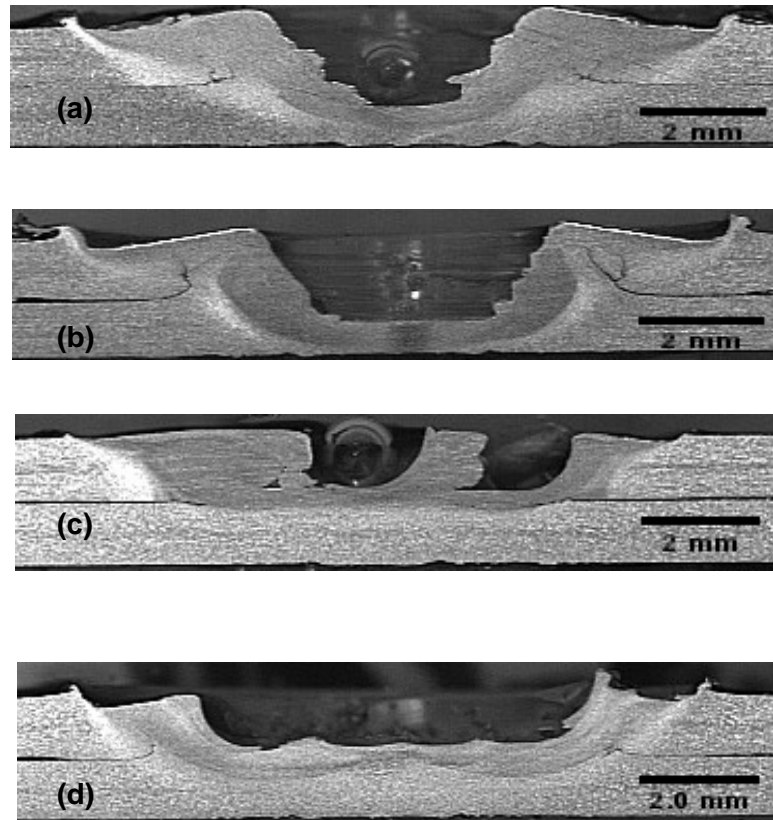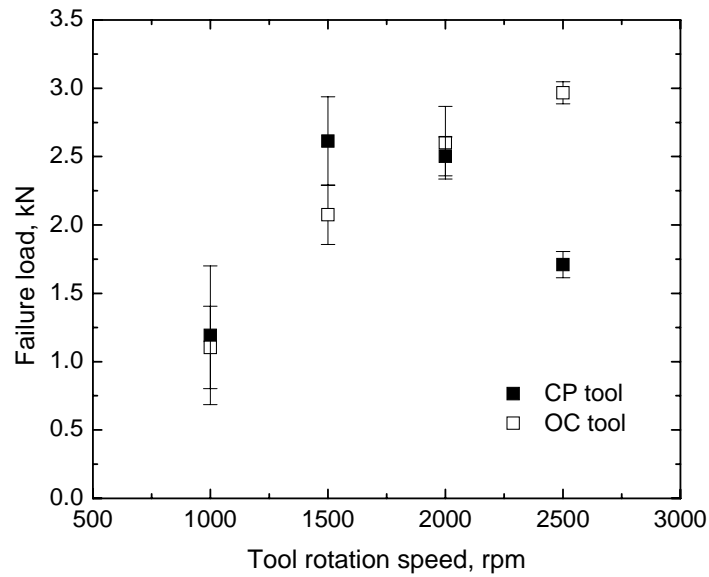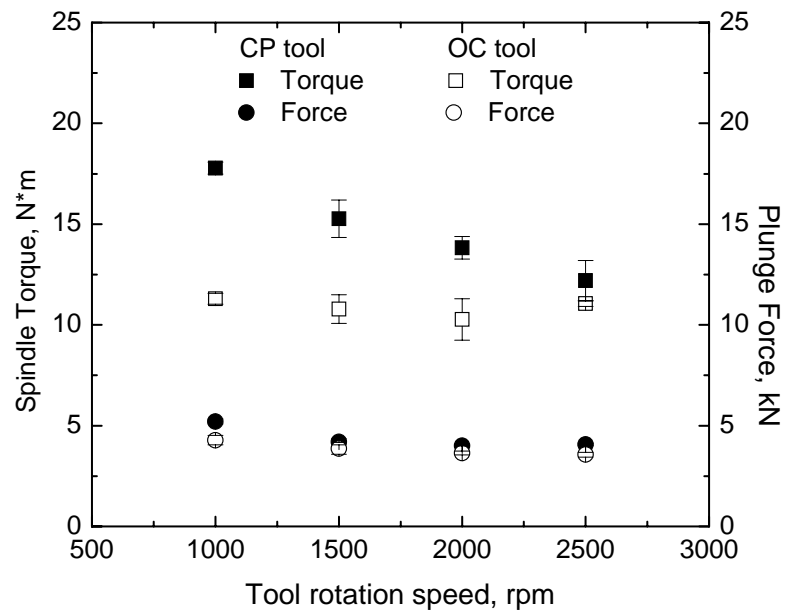Fig. 1.2. Macro images of (a) Conventional pin tool and (b) Off-center feature tool.

Fig. 1.3. Optical macrographs of spot welds made using conventional pin tool at (a) 1500 rpm and (b) 2500 rpm; off-center feature tool at (c) 1500 rpm and (d) 2500 rpm.
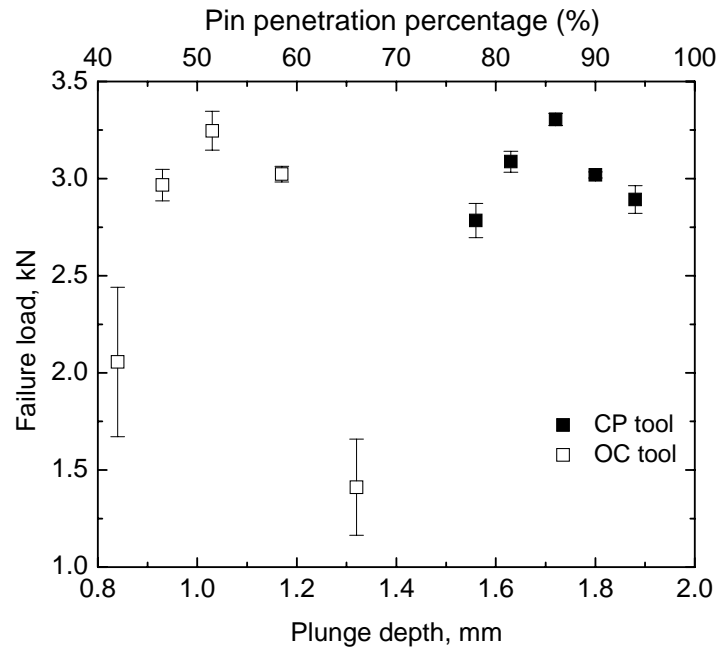
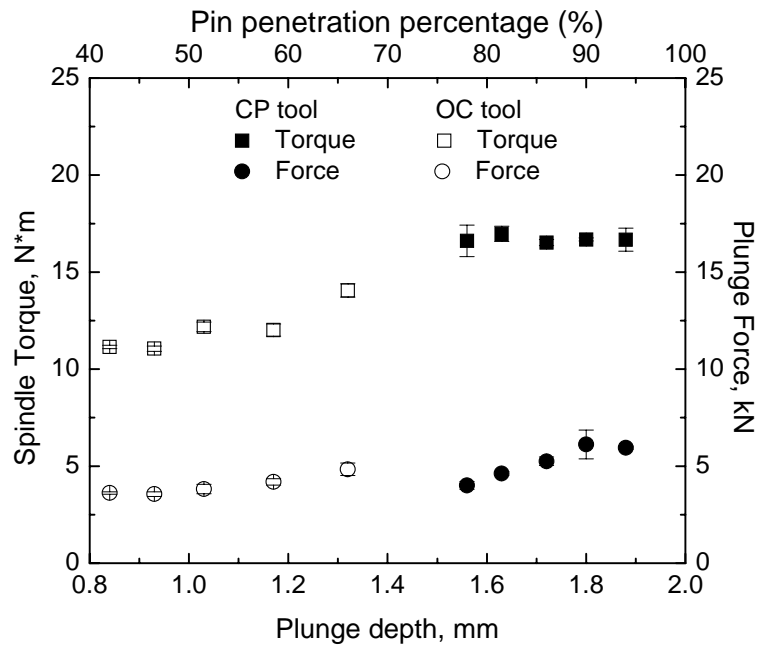(a) Lap-shear failure load as a function of tool rotation speed.

(b) Spindle torque and plunge force as a function of tool rotation speed.

Fig. 1.4. Effect of rotation speed on failure load, plunge force and spindle torque.
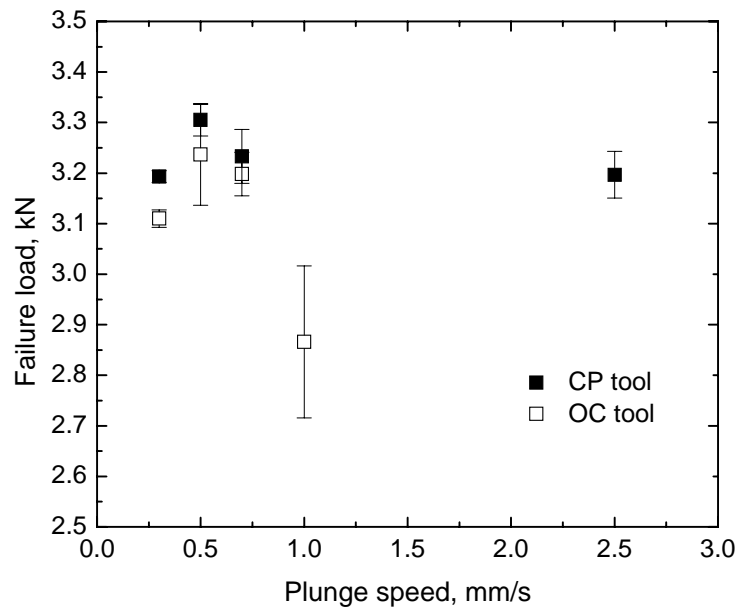
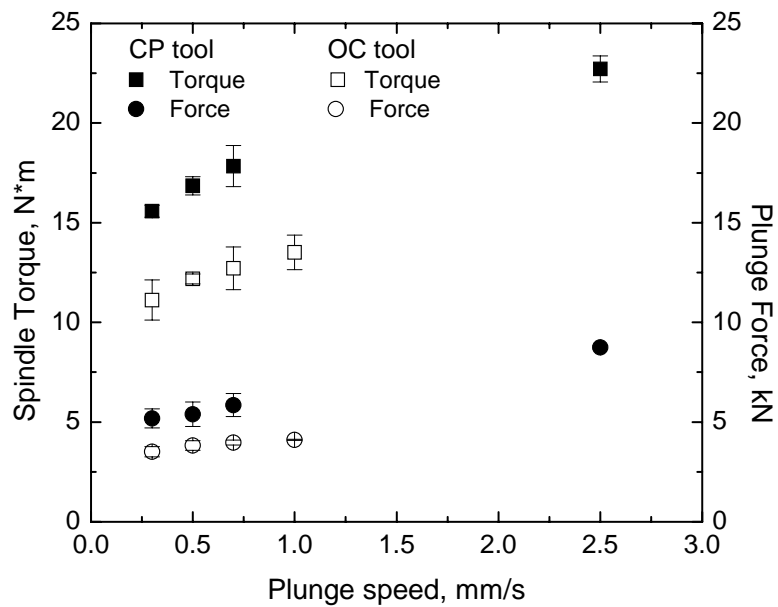(a) Lap-shear failure load as a function of plunge depth.

(b) Spindle torque and plunge force as a function of plunge depth.

Fig. 1.5. Effect of plunge depth on failure load, plunge force and spindle torque.
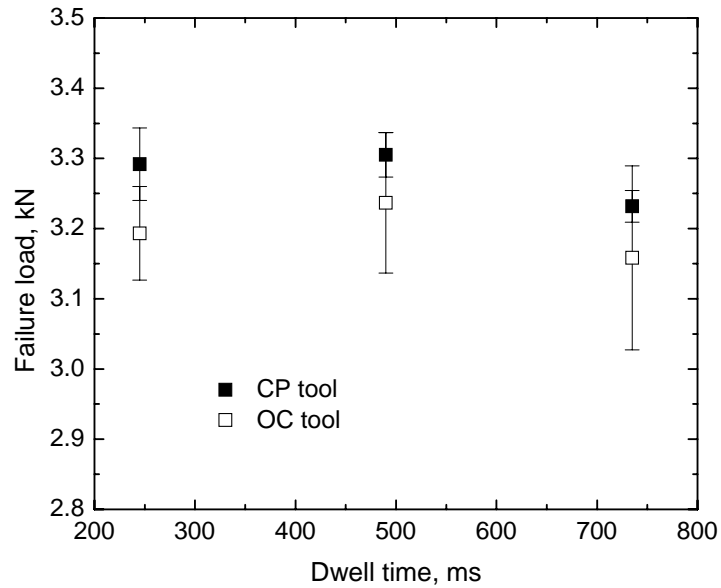
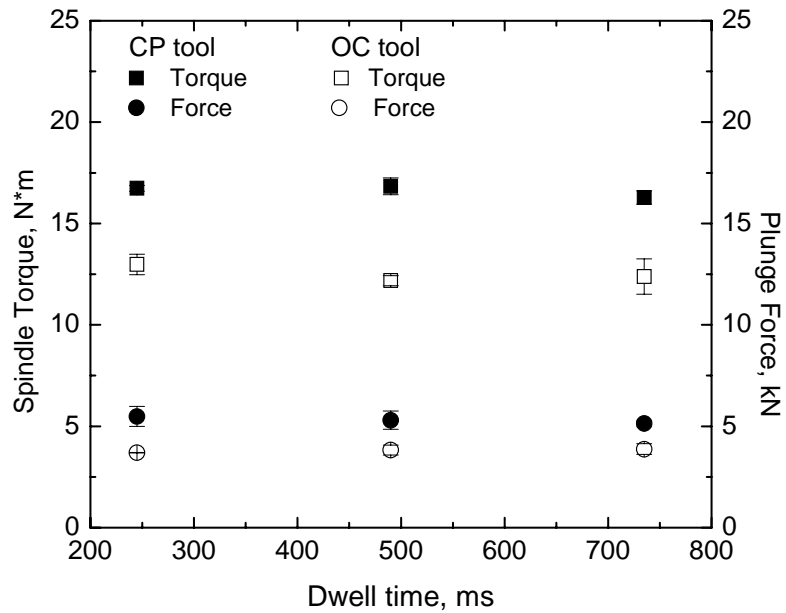(a) Lap-shear failure load as a function of plunge speed.

(b) Spindle torque and plunge force as a function of plunge speed.

Fig. 1.6. Effect of plunge speed on failure load, plunge force and spindle torque.

(a) Lap-shear failure load as a function of dwell time.

(b) Spindle torque and plunge force as a function of dwell time.

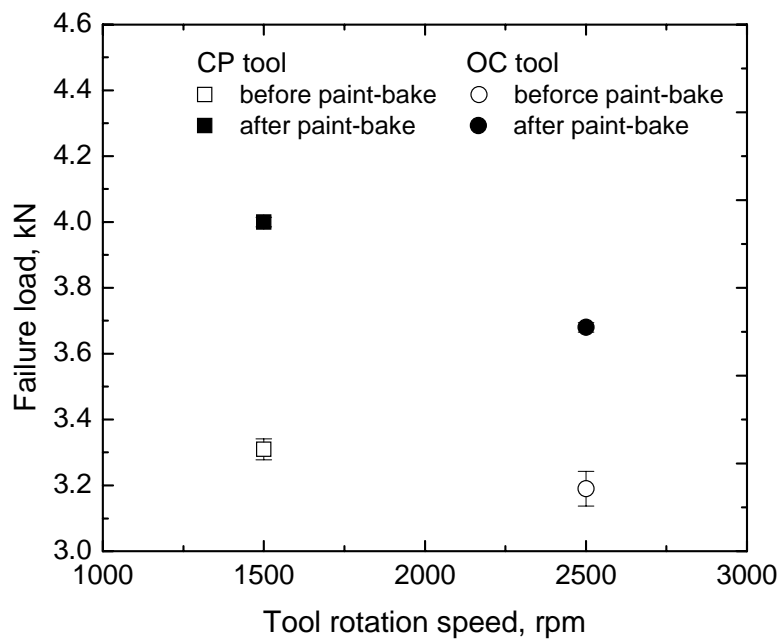Fig. 1.7. Effect of dwell time on failure load, plunge force and spindle torque.

Fig. 1.8. Effect of paint-bake cycle on lap-shear failure load.

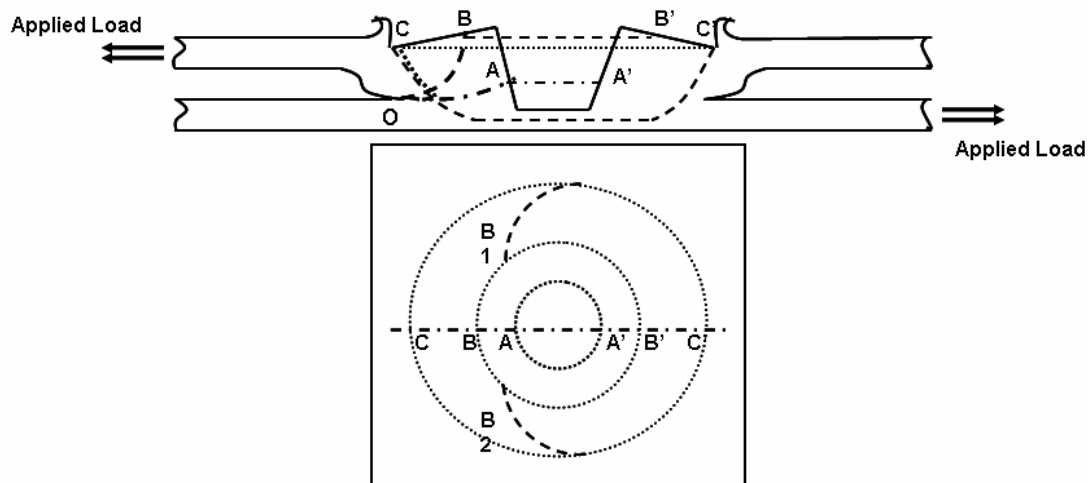Fig. 1.9. A schematic plot of failure modes for spot welds under lap-shear loading condition.
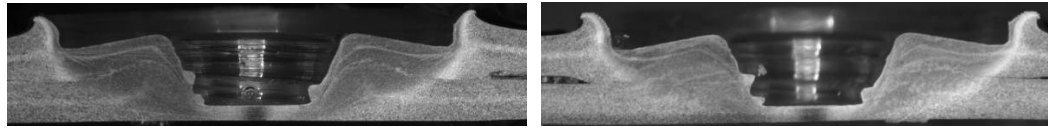
(a) Extension = 0   (b) Extension = 1 mm
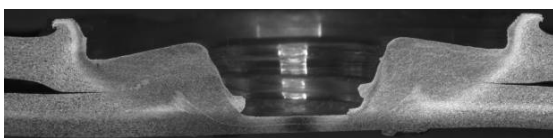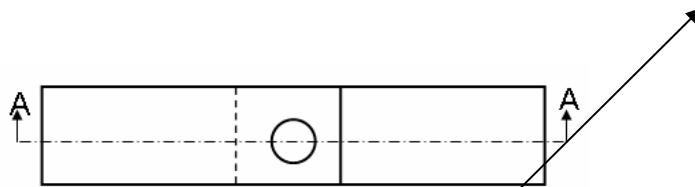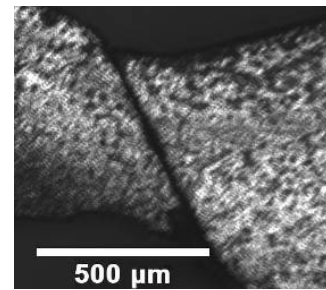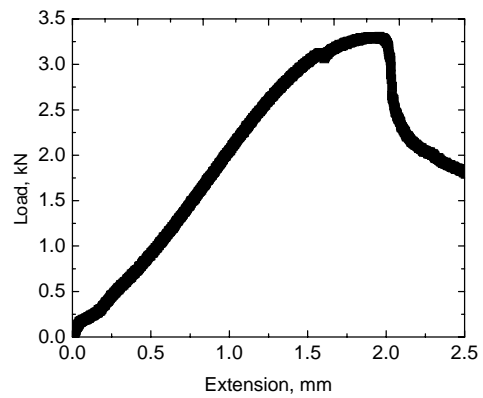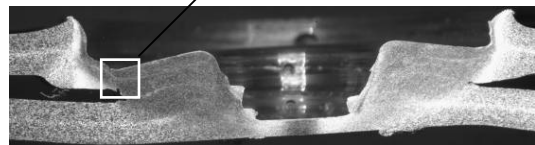
(c) Extension = 1.5 mm   (d) Extension = 2.0 mm

Fig. 1.10. Failure route of welds under mode USF condition.
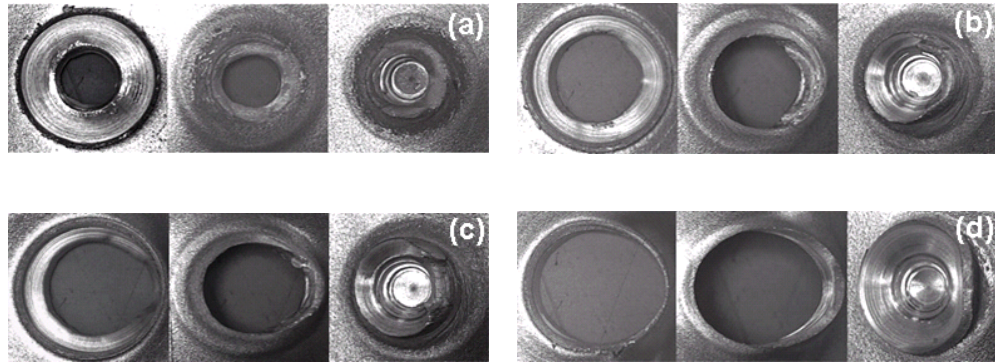
Fig. 1.11. Broken samples made using CP tool, failed by: (a) mode IF, (b) & (c) mode NF, and (d) mode USF. The photos show, from left to right, views of the top sheet, the underside of the top sheet and the bottom sheet.
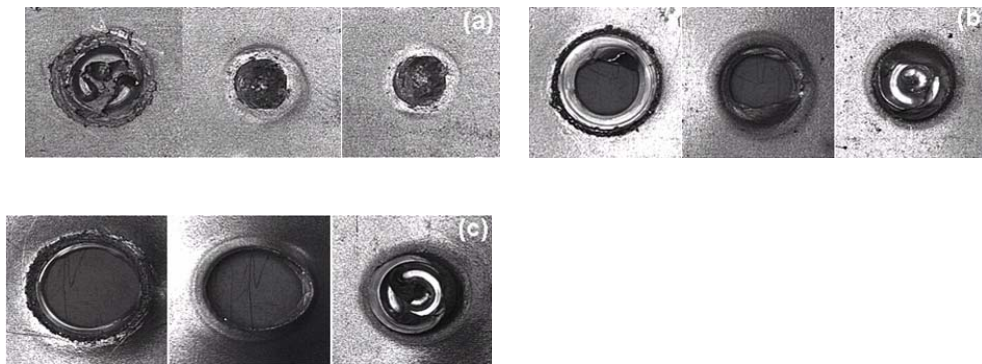
Fig. 1.12. Broken samples made using OC tool, failed by: (a) mode IF, (b) mode NF, and (c) mode USF. The photos show, from left to right, views of the top sheet, the underside of the top sheet and the bottom sheet.
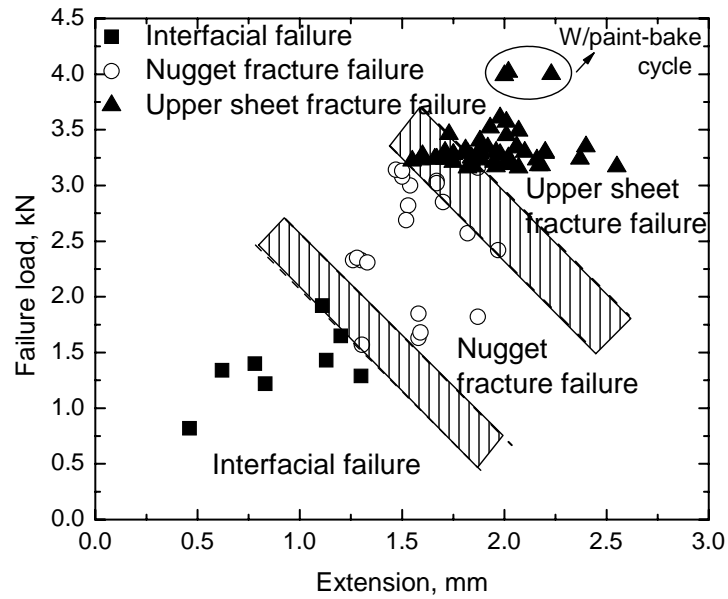
Fig. 1.13. Failure load as a function of extension for welds fail at different modes.
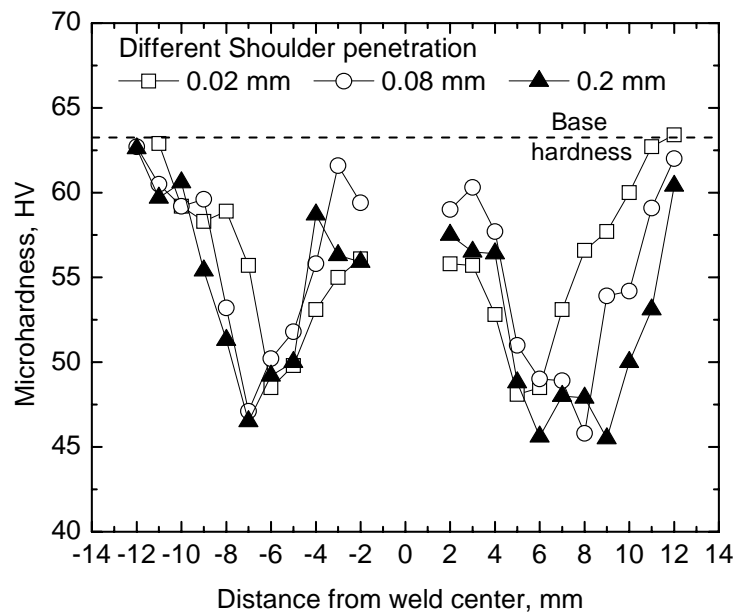
Fig. 1.14. Vickers microhardness distributions of welds at different shoulder penetration

depths.

II. MATERIAL FLOW DURING FRICTION STIR SPOT WELDING

W. Yuan, R.S. Mishra[*]

Center for Friction Stir Processing, Department of Materials Science and Engineering,

Missouri University of Science and Technology, Rolla, MO 65409, USA

(Prepared for publishing in Science and Technology of Welding and Joining)

ABSTRACT

Friction stir spot welds were made using a conventional step spiral pin tool. Material flow during friction stir spot welding (FSSW) was investigated by decomposing the welding process and examining dissimilar alloys spot welds. A skew "Y" shape oxide layer was formed during the welding process. The size of this oxide layer was reduced by decreasing tool rotation speed. Dissimilar spot welding of Aluminum alloy 6016 (AA6016)/AA5182 indicated that a thin upper sheet layer (38 to 142μm) was pushed under the tip of the rotating pin and retained as the pin penetrated into the bottom sheet. As the tool penetration depth increased, upper sheet material was transported downwards by pin steps and forging pressure applied by shoulder, while bottom sheet material was extruded and displaced upwards. A sandwich-like structure was formed when downward upper sheet and upward bottom sheets were incorporated at the top of the pin steps. The formation of lamella structure in the stir zone at high tool rotation speed was observed and discussed.

Keywords: Friction stir spot welding, material flow, dissimilar welding, aluminum alloy, shear layer

* Corresponding author. Tel: +01 573 341 6361 fax: +01 573 341 6934 E-mail: rsmishra@mst.edu (R.S. Mishra)

2.1. INTRODUCTION

A derivative of friction stir welding (FSW), which was developed by TWI, UK in 1991 as a novel method for joining aluminum alloys [1], FSSW is a solid-state welding technique. In such a process, a rotating tool with a protruding pin is plunged into the overlapping sheets to be joined and supported by a back-plate. After plunging a predetermined depth and a certain dwell time, it is retracted and a keyhole is left. The frictional heat generated at the tool-workpiece interface softens the surrounding material and the rotating and moving pin causes the material flow in both the circumferential and axial directions. The intermixing of the plasticized material and forging pressure on plasticized material applied by the tool shoulder result in the formation of a solid bond region [2, 3].

The detailed material flow during FSSW is quite complex and not fully understood. Welding parameters, tool geometry, and joint design exert significant effects on the material flow pattern and temperature distribution [4]. The properties of welds made by friction stir spot welding are directly related to the material flow around the tool. Material flow results in the formation of hooking feature and some oxide layers. The formation of these defects is obviously detrimental to shear and tension properties of joints [5, 6]. Proper understanding of the material flow during different stages of FSSW is essential to achieve optimized welding parameters and obtain high structural efficiency welds.

Numerous investigations on material flow behavior during FSW are reported and summarized by Mishra et al. [4] and Gerlich et al. [7]. The existing literature information on material flow during FSSW is limited. Su et al. [8] analyzed the material flow during spot welding of dissimilar AA5754/AA6111 and indicated a downward material flow in the location close to the tool periphery and an upward material flow within the stir zone further from the pin periphery. Tozaki [9] also provided a similar schematic illustration of

this material flow during spot welding of dissimilar AA 2017-T6 and AA5052. Muci-Kuchler et al. [10] analyzed the material flow during refill type FSSW by embedding 1100 aluminum rods in 7075-T73 plate at several radial locations from the center of the tool and indicated the material located directly underneath the pin or contact with the pin surface experienced a significant stirring motion. In addition, some computational methods including FEA have been also used to model the material flow [11-13].

Current literature results on material flow during FSSW are based on analysis or modeling of sound welds. The material flow in the early stage of plunge is not clear. However, some "defecting" welds with limited bonding are likely to give a better understanding of material flow. In the present paper, material flow during FSSW was illustrated by decomposing the welding process. AA5182 which was hard to etch for selected enchant was used to give a better contrast of hooking defect and some oxide layers formed during welding. Dissimilar welding of AA6016-T4 and AA5182 was performed to analyze the interaction of upper and bottom materials. Spot welding of similar AA6016 with copper strip marker lying between sheets was employed to investigate the material flow in the stir zone. The effect of step spiral pin and tool rotation speed on stir zone formation was also studied.

2.2. EXPERIMENTAL PROCEDURES

1.00 mm thick AA6016-T4 and 1.05 mm AA5182 aluminum alloy sheets were used in this study. The nominal compositions of AA6016 and AA5182 are indicated in Table 2.1. Aluminum sheets were sheared to a dimension of 38.1mm long and 25.4 mm wide for all spot welds.

Table 2.1. Nominal compositions of Al alloys used, wt%.

Material	Mg	Si	Mn	Cu	Fe	Al
Al 6016-T4	0.58	0.70	0.15	0.22	0.22	98.13
Al 5182	4.50	-	0.35	-	-	95.15

A plunge type FSSW machine with axial load capacity of 22.2 kN and counter-clockwise spindle rotation speeds up to 3000 rpm was used. The FSSW machine also had the capability to vary plunge speeds up to 25mm/s and dwell time up to a maximum of 1470 milliseconds (ms). During spot welding, axial force, torque and time were data logged. In present study, the spot welding machine was operated under a position control mode. A retract-then-stop mode was applied to all the welds made to keep a good surface appearance and reduce sticking of material under the pin tip.

Tool used in this study is shown in Fig. 2.1. It is a conventional tool with a step spiral pin, and has a concave shoulder with 10 mm diameter, and a 1.51 mm long pin length with the root diameter of 4.5 mm and tip diameter of 3 mm. The tool was machined from Densimet tungsten alloy.

Friction stir spot welds were made at various combinations of tool rotation speeds and plunge depths, while plunge speed and dwell time were held constant at 0.5mm/s and 490ms. During dissimilar spot welding, AA6016 sheet was placed on the top and AA5182 sheet at the bottom. The first mentioned alloy is designated as the upper sheet in dissimilar spot welding. The intermixing of sheet material was investigated by placing 0.06 mm copper strip as markers right under the center of tool between two AA6016 sheets before spot welding and tracking the debris in the stir zone.

During metallographic examination, all welds in each condition were cross-sectioned, mounted and etched using a 5% HF reagent to determine weld morphology. Cross sections were investigated by using a digital microscope camera and optical microscope. Since AA5182 is harder to etch than AA6016, the AA5182 was etched white and AA6016 was black as observed with digital camera. However, in an optical microscope, AA6016 was white and AA5182 was black.

2.3. RESULTS AND DISCUSSION

2.3.1. The Formation and Factors of a Skew "Y" Oxide Layer (AA5182/AA5182)

Fig. 2.2 shows the cross-section of AA5182 spot weld made at 1500 rpm tool rotation speed. A skew "Y" shape oxide layer was found in the stir zone. This oxide layer was different from most of the faying surface feature reported in current literature. Though similar feature can be noted in some papers [5-7, 14], the formation of this skew "Y" oxide layer was not elucidated.

The formation of this skew "Y" shape layer was first displayed and explained by decomposing the welding process. The tool was plunged into workpieces to different penetration depths. Fig. 2.3a indicates the rotating pin just penetrated the upper sheet. At the same time, the tool shoulder was not in contact with the toroid of upper sheet material which was expulsed and pushed upwards. Because of the support from bottom sheet, the softer upper sheet material from around and beneath the pin was ejected to the gap between two sheets. As shown in Fig. 2.3b, as the pin was plunged deeper into the sheets, the toroid of expulsed material increased in size and started to fill the cavity of the shoulder and the outer circumference of shoulder just contacted the surface of upper sheet. Soft bottom sheet material around pin was extruded upwards. Under the squeeze of extruded bottom sheet material and tool shoulder, the pre-ejected upper sheet material oriented and formed a skew "Y" shape layer by filling the gap between the two layers.

Further increase in the penetration depth resulted in the orientation change of skew "Y" layer. It also can be noted from Fig. 2.3c that the skew "Y" layer moved away from the welding center and the gap between two sheets was fully filled, because much more bottom sheet material was extruded by the rotating pin and forging pressure applied by tool shoulder. Compared with lower penetration depth welding in Fig 2.3a and 2.3b, a larger stir zone is apparent in Fig. 2.3c and 2.3d. This is likely a result of the additional frictional heat and further involvement and mixing of upper and bottom sheet material into the stir zone.

This continuous oxide layer was detrimental to joint properties, especially for lap-shear strength and cross-tension strength. Elimination or reduction of this oxide layer is likely to improve the weld properties. As discussed above, the length of skew "Y" oxide layer was correlated to the volume of pre-ejected upper sheet material which was determined by the pin volume. The conical pin feature and the ratio of pin length to upper sheet thickness also played a role in the material ejected.

The pin volume had a great effect on the material displaced, however, it should be mentioned that the volume of displaced material was less than that of pin volume, because some soft material would become flash. The volume of pre-ejected upper sheet material correlates with its softness and pressure applied on it. The conical pin feature would also affect the distribution of pressure applied on the displaced material. This might be the reason why skew "Y" oxide layer formation was not observed when using cylindrical pin feature in current literature. The step spiral pin tool is likely to exert a sideward force component to the displaced material, which is then likely to insert in the gap between the two sheets. The ratio of pin length to upper sheet thickness also had an effect on skew "Y" oxide layer formation. For small ratios, the shoulder would squeeze

workpieces before soft material displaced into the gap region; then the skew "Y" oxide layer would lose its outer branch that was far away from the pin hole.

All the factors mentioned above aim to reduce the volume of displaced material and they do not change for particular tool design and workpieces. The flexible factors that would affect material flow are welding parameters. Previous work has shown that lower tool rotation speeds gave higher weld properties [2,15] for this conical step spiral pin feature tool. Fig. 2.4 shows the cross-sections and microstructures of spot welds of AA5182 made at 1000 rpm and 3000 rpm tool rotation speeds. It can be seen that, at low rotation speed, the branches of "Y" layer were limited and optical microstructure indicated the inner branch of "Y" layer was dispersive and became discontinued. At high rotation speed, the skew "Y" layer was displaced upwards and two branches were closer. Though the upward movement of faying surface was far away from the welding center at high rotation speed, the layer was continued into the stir zone. Compared with 1000 rpm tool rotation speed, bottom sheet material underwent a severe plastic deformation at 3000 rpm rotation speed.

Although, formation and evolution of oxide layer was observed, the interaction between upper and bottom sheet was not clear, especially for the stir zone, dissimilar aluminum alloy spot welding was used to help visualization of material flow based on their differing etching characteristics.

2.3.2. The Interaction of Upper and Bottom Sheet Materials (AA6016/AA5182)

Fig. 2.5 shows the cross section and microstructures of dissimilar AA6016/AA 5182 spot weld made at 1500 rpm tool rotation speed and 0.2 mm shoulder penetration depth. A layer of upper sheet material (AA6016) close to pin periphery was moved downward as the pin penetrated into the bottom sheet (AA5182). At the same time, the bottom sheet

material was displaced upwards outside the upper sheet material that flowed downwards. The thread-like configuration on the displaced bottom sheet material shown in Fig. 2.5b might indicate the rotation cycles it underwent during pin penetration.

Based on the optical microscopy, a thin layer of bottom sheet material was pushed beneath the pin tip with about 40 μm thickness under the center of pin tip; however, the thickness of this layer varied from 70 μm to 120 μm close to the periphery of pin tip. Fig. 2.6 shows the thickness of upper sheet layer that was pushed beneath the pin tip at different tool rotation speeds and penetration depths. The thickness of layer varied from 38 μm to 142 μm for 1500 rpm tool rotation speed, and 21μm to 28 μm for 2500 rpm tool rotation speed. Su et al. [8] reported similar layer during dissimilar welding of AA5754/AA6111, with unchanged thickness about 140μm as tool penetration continued into the bottom sheet and indicated that this layer resulted from a formation of dynamically quiescent region where the fluid flow was of the order of micrometers per second. Different tool designs and process parameters used might be the reasons for the difference of layer thickness reported.

Fig. 2.7 shows the cross sections of welds made at 1500 rpm and 2500 rpm with three different plunge depths. The volume of displaced bottom sheet material increased as the penetration depth increased for both tool rotation speeds. Tozaki et al. [14] showed similar results by increasing pin length and keeping shoulder penetration depth constant as 0.2 mm. At the same time, more and more upper sheet material was transported to the stir zone due to increased forging pressure applied by shoulder and counts of pin rotation. Compared with lower rotation speeds, higher rotation speeds resulted in high frictional heat and pin rotating cycles, thus more upper sheet material was transported into the stir zone, even at a shallower plunge depth.

2.3.2.1. Upward material flow

For both rotation speeds, as the penetration depth increased, the displaced bottom sheet material flowed upwards and back into the stir zone. As shown in Fig. 2.8 at 2500 rpm tool rotation speed, a sandwich-like structure was formed when downward upper sheet and upward bottom sheets were incorporated at the top of pin steps. It was suggested that a shear layer of material beneath the shoulder and around the pin rotated with tool. The volume of this layer varies with the change of conditions at the tool-workpiece interface between stick and slide [16-18]. Su et al. [8] reported an upward material flow with anticlockwise spiral motion by incorporating Al_2O_3 particle traces into the stir zone formed during Al 6061-T6 spot welding.

2.3.2.2. Downward material flow

One of the possibilities that upper sheet material moved down as tool penetrated into the bottom sheet was pin step. Fig. 2.7 shows the upper sheet material was trapped at the pin steps and moved downwards with rotating pin. It was expected that the material transported downwards also with a spiral movement which was consistent with the tool rotation. Another possibility was frictional contact between the base of concave tool shoulder and upper sheet material. It can be noted from Fig. 2.5b that the displaced bottom sheet material was dragged or pushed down at a distance of 250μm away from the pin periphery. An upper sheet layer around the pin was also found during AA5754/AA6111 spot welding when using smooth unthreaded pin [19], which indicated that the pin step or thread was not the only reason to transport material from top to bottom.

Upper and bottom sheet material were incorporated at the top of the steps of the rotation pin. However, intermixing of these sheets in the stir zone was not observed.

2.3.3. The Mixing in Stir Zone (AA6016/Cu strip /AA6016)

Fig. 2.9 shows the cross section of spot weld of AA6016/Cu strip /AA6016 at 1500 rpm tool rotation. 0.06 mm Cu strip was placed between the Al 6016 sheets with the bottom side sticky to the bottom sheet before spot welding. A large piece of Cu debris was found adjacent to shoulder indentation and close to the root of the pin. At the same time, some smaller Cu debris was observed below faying surface and close to the pin periphery which was the mixing zone. The dark region indicated in the cross section was glue. Under the pin tip, a layer of sheet material was observed above the glue boundary. On the other hand, this glue at the outer extremity of the retention upper sheet layer demonstrated that this layer was inactive when pin penetrated into the bottom sheet, which verified the formation of dynamically quiescent region. The observation of Cu debris in stir zone indicated there was a intermixing between upper and bottom sheet material during spot welding.

2.3.4. The Effect of Tool Rotation Speed on Stir Zone Formation for Step Spiral Pin

The critical role that the step spiral pin feature and tool rotation speeds play in terms of facilitating intermixing during AA6016 spot welding is shown in Fig. 2.10. The morphology of stir zone was quite different. A large stir zone was found at 1000 rpm tool rotation speed with discontinue and dispersed oxide. However, for 3000 rpm tool rotation speed, lamella pattern was observed in the stir zone which was smaller and limited to the region around the rotating pin. The skew "Y" oxide layer was found and continued into the region close to pin periphery.

Fig. 2.11 shows force, torque plots during spot welding at two different tool rotation speeds. It can be seen that, the spindle torque was much higher at 1000 rpm tool rotation speed than that at 3000 rpm rotation speed. As the tool rotation speed increased, the temperature of the weld sheet increased material around the pin and under the shoulder

became softer and easier to flow. Then the torque was reduced and less heat was generated by mechanical work. Integration of torque curves indicated that much more mechanical work was input at lower rotation speed. When ignoring the heat loss, much more material should be deformed at 1000 rpm tool rotation speed.

A rotating layer of forging zone beneath tool shoulder and extrusion zone around the pin were indicated during friction stir welding [17]. It was reported that the interaction between weld tool and workpiece during friction stir welding may alternate between stick and slide to stabilize the temperature and avoid melting of the welding material [16]. At lower temperature, the deformation flow stress is higher, plastic material is easier to stick to the shoulder and around the pin. At higher temperature with lower material deformation flow stress, the slide interaction occurs. This explained higher plastic deformation at low tool rotation speed.

The lamella structure formed in the stir zone was only observed at 3000 rpm rotation speed, shown in Fig. 2.12. The formation of this structure might be because of the difference in the flow properties of material under the shoulder and around the pin and pin steps which transport material. It was suggested that a hot shear layer formed under the shoulder and around the pin at high tool rotation speed [16]. Material close to the top of pin step was transported downwards to the pin tip, and then it was discharged from the bottom of the pin and displaced upwards. With low flow stress in the shear layer around the pin at high temperature, the displaced material moved back towards the pin periphery and got mixed with the downward material flow, and then the mixed material was again transported to the pin tip.

2. 4. CONCLUSIONS

Material flow during friction stir spot welding with conventional step spiral pin was investigated by decomposing the welding process and examining dissimilar alloys spot welds, which allowed a visualization of material flow based on their differing etching characteristics. A skew "Y" shape oxide layer was formed during the welding process. The size and formation of this oxide layer could be reduced or eliminated by varying process parameters and tool design. The size of this layer was reduced greatly at low rotation speed (1000 rpm). Dissimilar spot welding of AA6016/AA5182 indicated a 38 to 142 μm upper sheet layer under the tip of the rotating pin and retained as the pin penetrated into the bottom sheet. Upper sheet material was transported downwards by pin steps and shoulder forging pressure, while bottom sheet material was extruded and displaced upwards. The upward and downward flow got mixed at the top of pin step and a sandwich-like structure formed. Lamella structure in the stir zone was observed at high tool rotation speed which indicated the material transported to the pin tip was discharged and moved back towards the pin periphery repeatedly.

2.5. ACKNOWLEDGMENTS

2.6 REFERENCES

[1]   W. M. Thomas, E. D. Nicholas, J. C. Needham, M. G. Murch, P. Templesmith, C. J. Dawes, G. B. Patent 9125978.8 (1991).

[2]   T. Freeney, S. R. Sharma, R. S. Mishra, SAE Technical paper (2006) 2006-2001-0969.

[3]   S. Lathabai, M. J. Painter, G. M. D. Cantin, V. K. Tyagi, Scripta Materialia 55 (2006) 899-902.

[4]   R. S. Mishra, Z. Y. Ma, Materials Science and Engineering: R: Reports 50 (2005) 1-78.

[5]   P. Su, A. Gerlich, T. H. North, SAE Technical paper (2005) 2005-2001-1255.

[6]   M. Valant, E. Yarrapareddy, R. Kovacevic, International Trends in Welding Research Conference, May 16-20 (2005).

[7]   A. Gerlich, P. Su, M. Yamamoto, T. H. North, Science and Technology of Welding and Joining 13 (2008) 254-264.

[8]   P. Su, A. Gerlich, T. H. North, G. J. Bendzsak, Science and Technology of Welding and Joining 11 (2006) 61-71.

[9]   Y. Tozaki, Y. Uematsu, K. Tokaji, Fatigue & Fracture of Engineering Materials & Structures 30 (2007) 143-148.

[10] K. H. Muci-Kuchler, S. K. Itapu, W. J. Arbegast, K. J. Koch, SAE Technical paper (2005) -01-3323.

[11] K. H. Muci-Küchler, S. S. T. Kakarla, W. J. Arbegast, C. D. Allen, SAE Technical paper (2005) 2005-2001-1260.

[12] M. Awang, V. H. Mucino, Z. Feng, S. A. David, SAE Technical paper (2005) 2005-2001-1251.

[13] S. S. T. Kakarla, K. H. Muci-kuchler, W. J. Arbegast, C. D. Allen, TMS (2005)

[14] Y. Tozaki, Y. Uematsu, K. Tokaji, International Journal of Machine Tools and Manufacture 47 (2007) 2230-2236.

[15] R. S. Mishra, T. A. Freeney, S. Webb, Y. L. Chen, D. R. Herling, G. J. Grant, Friction Stir Welding and Processing IV, TMS (2007).

[16] J.A. Schneider, in: R.S. Mishra, M.W. Mahoney (Eds.), Friction Stir Welding and Processing, ASM International, Ohio, 2007, 37-49.

[17] W. J. Arbegast, Scripta Materialia 58 (2008) 372-376.

[18] J. Schneider, R. Beshears, A. C. Nunes, Materials Science and Engineering a-Structural Materials Properties Microstructure and Processing 435 (2006) 297-304.

[19] P. Su, A. Gerlich, T. H. North, G. J. Bendzsak, Metallurgical and Materials Transactions a-Physical Metallurgy and Materials Science 38A (2007) 584-595.
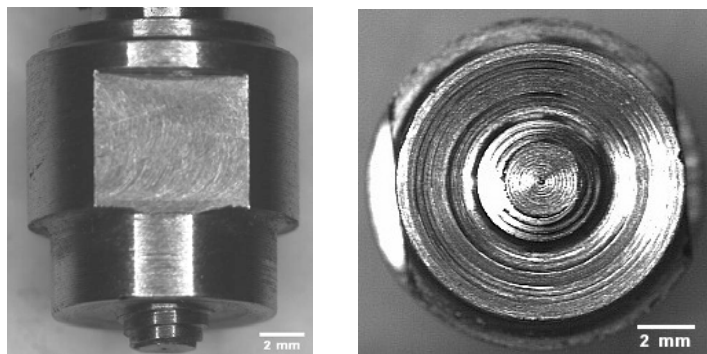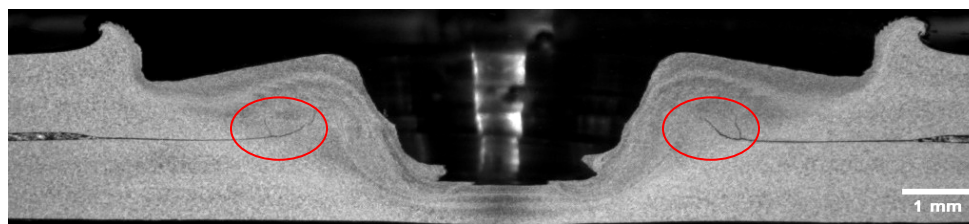
Fig. 2.1. Macro images of convention step spiral tool.

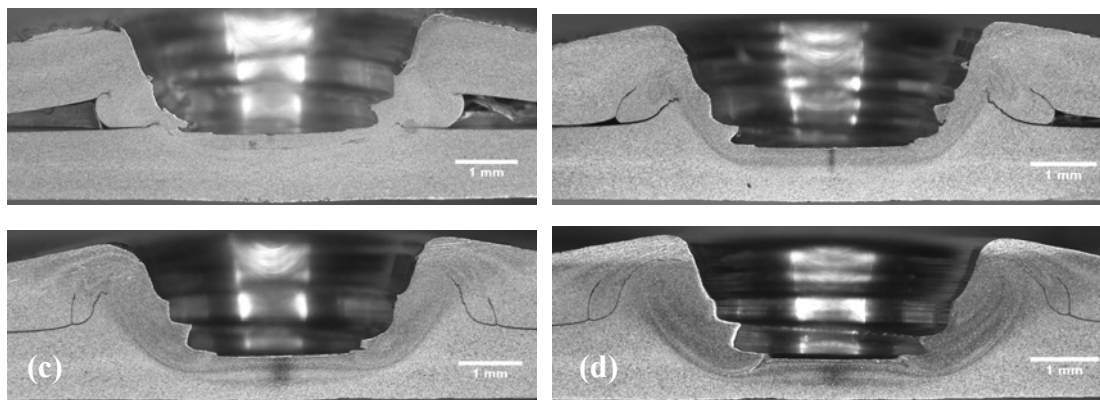Fig. 2.2. Optical macrograph of AA5182 spot weld made at 1500 rpm rotation speed.

Fig. 2.3. Optical macrographs of AA5182 spot welds made at 1500 rpm rotation speed,
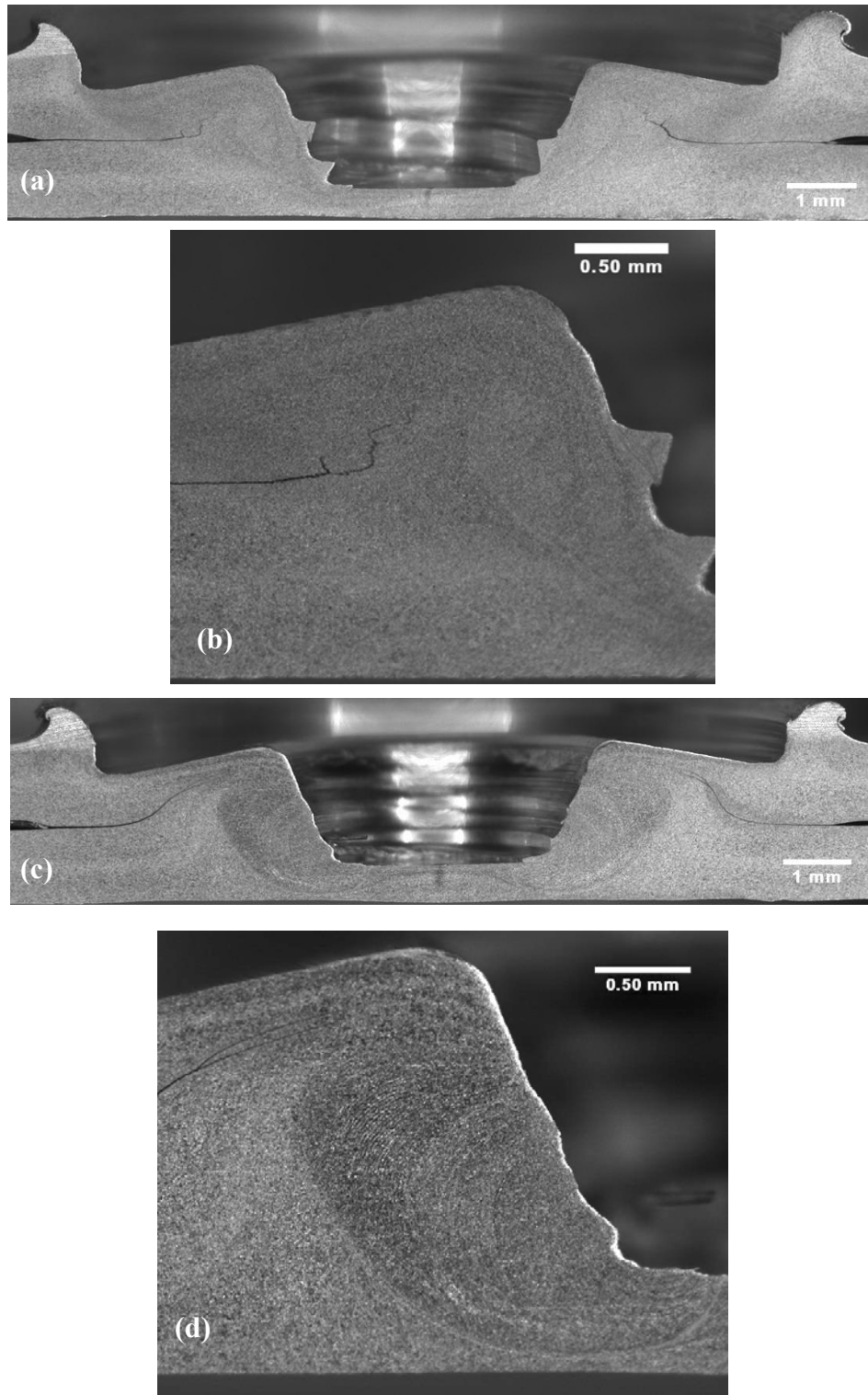different penetration depths. Penetration depth increases from (a) to (d).

Fig. 2.4. Optical macrographs and microstructures of AA5182 spot welds made at: 1000 rpm for (a), (b); 3000 rpm for (c), (d).
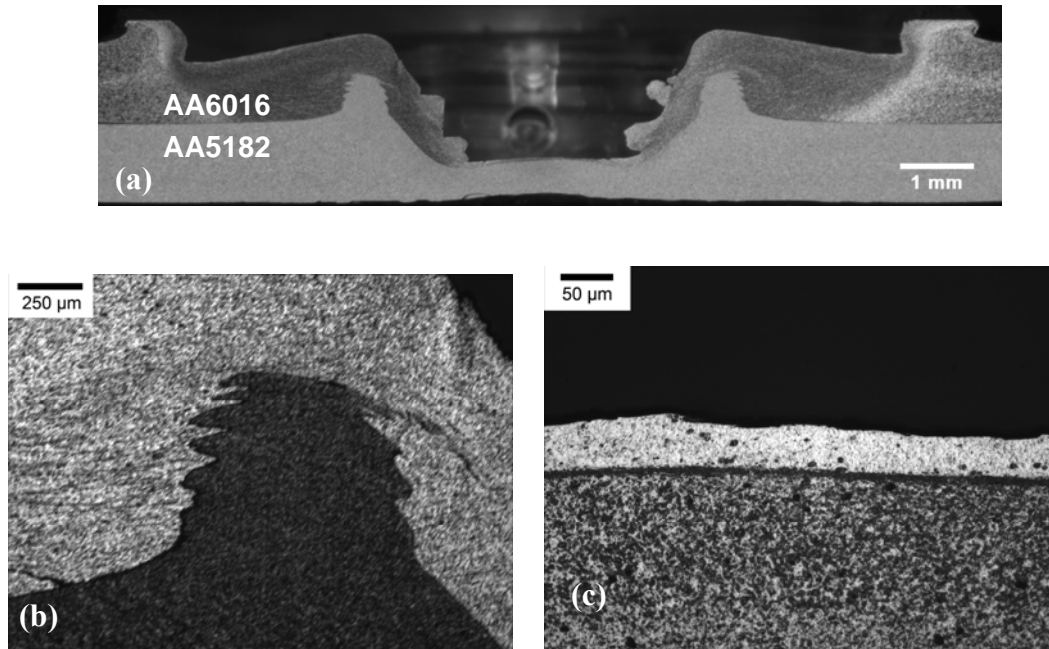
Fig. 2.5. Cross section and microstructures of AA6016/AA5182 spot weld.
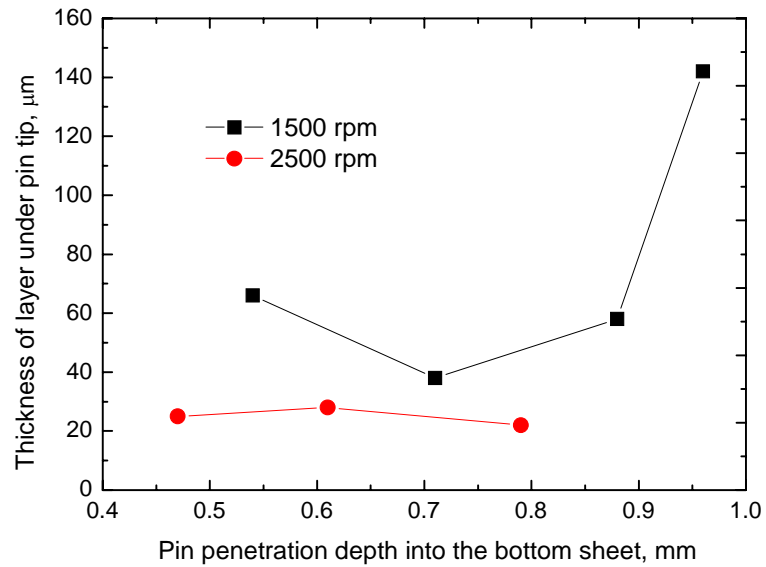

Fig. 2.6. Thickness of upper sheet layer under pin tip.

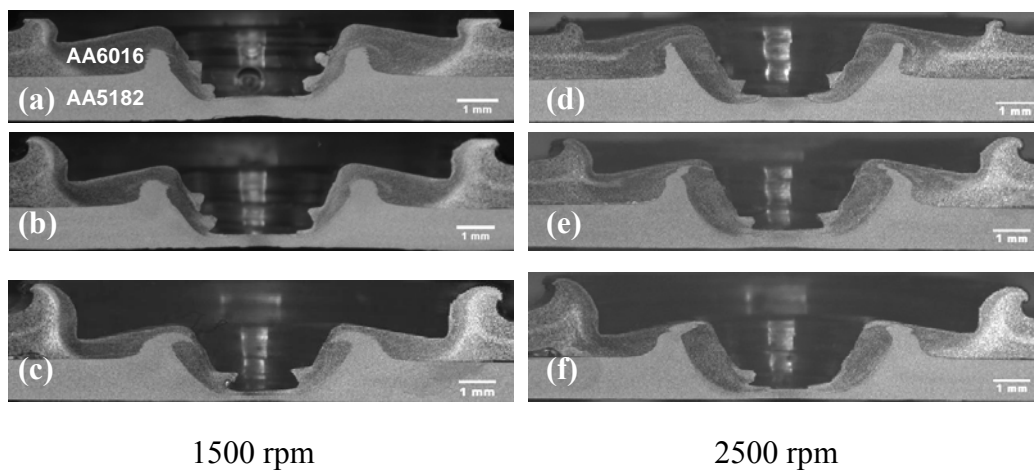1500 rpm   2500 rpm
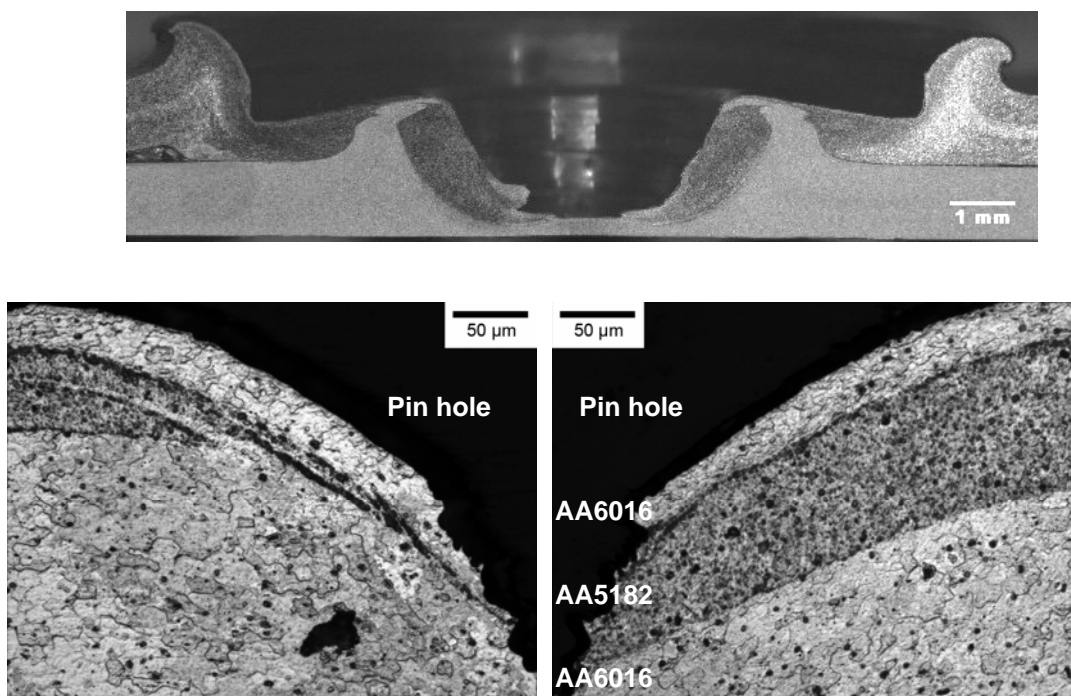
Fig. 2.7. Cross sections of dissimilar spot welds.
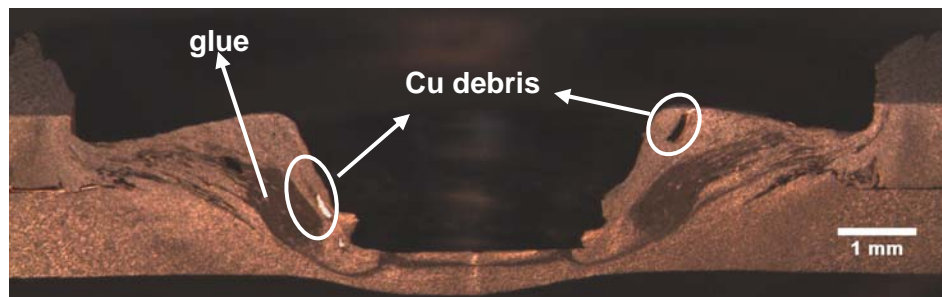

Fig. 2.8. Bottom sheet material flowed back into the stir zone.

Fig. 2.9. Optical macrograph of cross section of AA6016/Cu strip spot welding.
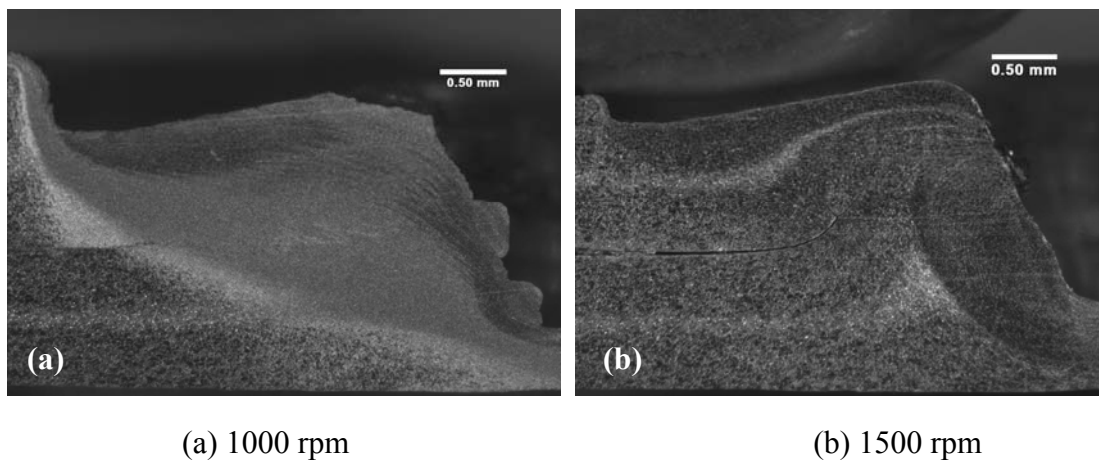

(a) 1000 rpm

(b) 1500 rpm

Fig. 2.10. Optical macrographs of cross sections of AA6016 spot welds.
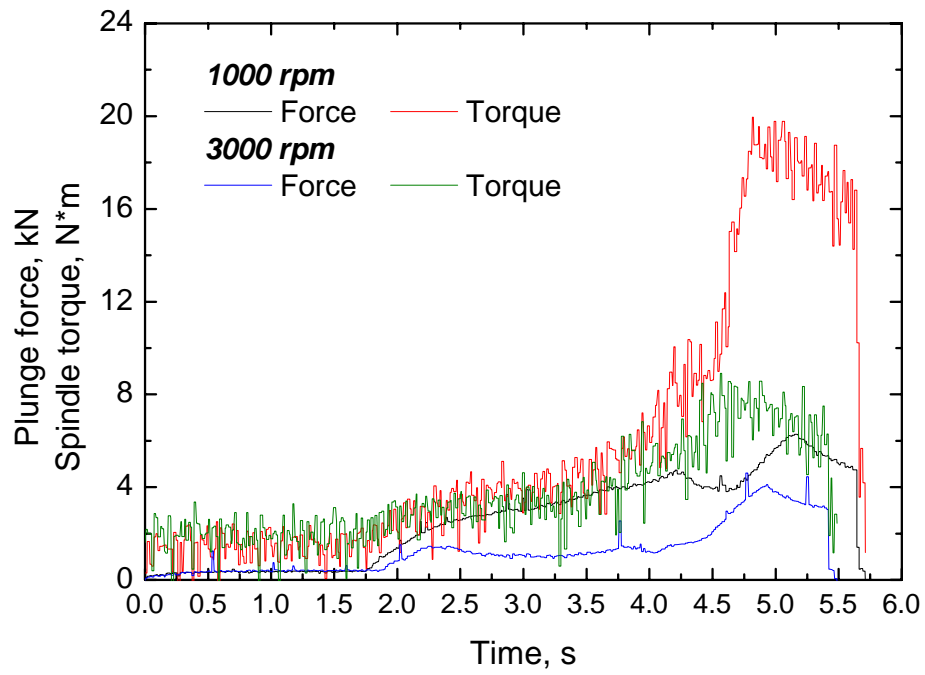
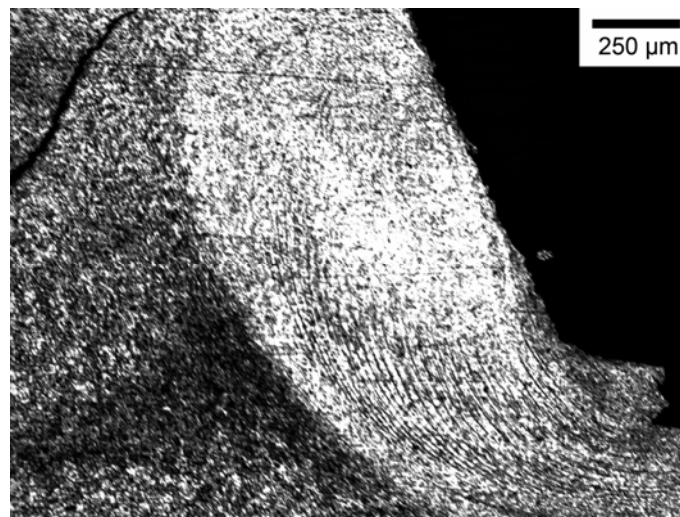Fig. 2.11. Plunge force and spindle torque during AA6016 spot welding.

Fig. 2.12. Lamella structure at 3000 rpm rotation speed.

2. CONCLUSIONS AND RECOMMENDATIONS

2.1. CONCLUSIONS

Conventional pin (CP) tool and off-center feature (OC) tool were compared for friction stir spot welding of 1mm thick commercial aluminum alloy 6016-T4 sheets. Tool rotation speed and plunge depth profoundly influenced lap-shear strength of welds. For both tools, plunge force and spindle torque increased as tool rotation speed decreased or tool penetration depth increased.

Both tools exhibited a maximum weld failure load of about 3.3 kN, which was much higher than strength (1.3 kN) specified in MIL-W-6858. Paint-bake cycles increased weld strength by 20.8% and 15.4% for CP tool and OC tool, respectively. Optimized parameters achieved for CP tool are 1500 rpm, 0.5mm/s plunge speed, 0.2 mm shoulder penetration depth and 490 ms dwell time, and for OC tool are 2500 rpm, 0.5mm/s plunge speed, 0.2 mm shoulder penetration depth and 490 ms dwell time. OC tool displayed much lower plunge force and torque.

CP tool gave lower lap-shear strength at higher tool rotation speed. This corresponded with the formation of larger and continuous "Y" type oxide layer at higher tool rotation rate. The size of this oxide layer was reduced at lower tool rotation rate. Three different failure modes were proposed; interfacial failure, nugget fracture failure and upper sheet fracture failure.

Dissimilar spot welding of AA6016/AA5182 indicated that upper sheet material was transported downwards by pin steps and shoulder forging pressure, while bottom sheet material was extruded and displaced upwards. The upward and downward flow got mixed at the top of pin step and formed a sandwich-like structure. Lamella structure in

the stir zone indicated the material transported to the pin tip was discharged and moved back towards the pin periphery repeatedly.

2.2. CONTRIBUTIONS

The purpose of this work was to compare different tool designs, evaluate process parameters on spot weld properties, and understand the material flow during FSSW. The main contributions of this research on friction stir spot welding of aluminum alloy are listed below:

➢ A design of off-center pin features. This unsymmetrical pin design reduced the plunge force and spindle torque greatly, but with similar weld properties. It also has a stronger ability to disrupt and further mix the oxide layer on the alloy surface. This could be used for welding dissimilar alloys with intermetallic compound formation on the faying surface.

➢ Classification of three lap-shear failure modes has been developed. It could be a guideline for achieving best weld properties. Since higher failure load was always shown in upper sheet fracture mode.

➢ The effect of paint-bake cycle on weld strength has been investigated. This could serve as a reference for automotive applications where paint-bake cycle is an integral part of manufacturing.

➢ Material flow during FSSW indicated lower rotation rates were better for achieving higher weld strengths for step spiral pin tool. Optimization of process parameters for spot welding using other aluminum alloys will be on similar lines when similar tool designs are used.

2.3. RECOMMENDATIONS FOR FUTURE WORK

Based on the experience gained in this research, the following recommendations for future work are suggested:

- Though numerous welds have been tested at various parameter combinations, the investigation of microstructural change was not done much, especially for precipitate evolution in heat treatable alloys during FSSW. TEM, DSC and some modeling work in the stir zone will be good for understanding the differences among different parameter combinations and the effect of paint-bake cycle on properties, since the amount and distribution of precipitates will vary with change of heat input to the alloy.

- The off-center feature gave further mixing of sheet material. It is still not clear how the off-center pin feature affects the material flow in detail. Though this is going to be a difficult work, material flow during FSSW using off-center feature pin will be helpful to understand the mechanism behind it.

VITA

Wei Yuan was born on June 25, 1984, in Anhui, China. He received his Bachelor of Engineering degree in Materials Science and Engineering from Southeast University, China, in June 2006. He came to USA in August 2006 for pursuing his masters. In August 2008, he received his Master of Science degree in Material Science and Engineering from Missouri University of Science and Technology (formerly University of Missouri-Rolla).